Development of a Detailed Surface Chemistry Framework in DSMC

Krishnan Swaminathan-Gopalan,[*]

Department of Mechanical Science and Engineering, University of Illinois at Urbana-Champaign, Urbana, IL, 61801, USA.

Arnaud Borner,[†]

Science and Technology Corporation at NASA Ames Research Center, Mail Stop 258-6, Moffett Field, CA, 94035, USA.

and Kelly A. Stephani[‡]

Department of Mechanical Science and Engineering, University of Illinois at Urbana-Champaign, Urbana, IL, 61801, USA.

A generalized finite-rate surface chemistry framework incorporating a comprehensive list of reaction mechanisms is developed and implemented into the direct simulation Monte Carlo (DSMC) solver SPARTA. The various mechanisms include adsorption, desorption, Eley-Rideal (ER), and several types of Langmuir-Hinshelwood (LH) mechanisms. The approach is to stochastically model the various competing reactions occurring on a set of active sites. Both gas-surface (e.g., adsorption, ER) and pure-surface (e.g., desorption) reaction mechanisms are incorporated, and the framework also includes catalytic or surface altering mechanisms involving the participation of the bulk-phase species (e.g., bulk carbon atoms). Marschall and MacLean developed a general formulation in which multiple phases and surface sites are used and a similar convention is adopted in the current work. Expressions for the microscopic parameters of reaction probabilities (for gas-surface reactions) and frequencies (for pure-surface reactions) that are required for DSMC are derived from the surface properties and macroscopic parameters such as rate constants, sticking coefficients, etc. The energy and angular distributions of the products are specified according to the reaction type and input parameters. This framework also presents physically consistent procedures to accurately compute the reaction probabilities and frequencies in the case of multiple reactions. The result is a modeling tool with a wide variety of surface reactions characterized via user-specified reaction rate constants, surface properties and parameters.

Nomenclature

A, B	chemical species in the gas phase
$A(s), B(s)$	chemical species adsorbed on the surface
A_v	Avogadro's number
E	Energy, J;Jmol^{-1}
E_a	Activation energy of reaction, J;Jmol^{-1}
E_b	Energy of desorption barrier, J;Jmol^{-1}
F_N	ratio of real to simulated particles in DSMC
f	Distribution function
h	Planck's constant, Js
K	equilibrium constant
k	reaction rate constant
k_b	Boltzmann's constant, JK^{-1}
$M(b)$	bulk species on the surface
m	mass, kg
N_A	total number of species A
n_A	surface number density of species A, m^{-2}
P	Probability
Rn	Uniform random number between 0 and 1
r	Rate of reaction
S	Sticking coefficient
S_0	Sticking coefficient at zero surface coverage
S_p	Area of surface element, m^2

---

[*]Graduate Research Assistant, Student Member AIAA.

[†]Research Scientist, Member AIAA.

[‡]Assistant Professor, Associate Fellow AIAA.

(s)	empty surface site
T	Temperature, K
t	time, s
u, v	velocity, ms^{-1}
$u_0, \bar{v}$	mean velocity, ms^{-1}
v_n	velocity along the surface normal, ms^{-1}

Abbreviations

AA	Associative Adsorption
AD	Adsorption-mediated GS reactions
ad	adsorption
CFD	Computational Fluid Dynamics
$CD, cond$	Condensation
DA	Dissociative Adsorption
DI	Direct Impact GS reactions
$DSMC$	direct simulation Monte Carlo
DS, des	desorption
EDF	Energy distribution function
ER	Eley-Rideal reaction mechanism
IS	impulsive scattering
LH	Langmuir-Hinshelwood reaction mechanism
MB	Maxwell-Boltzmann
max	maximum
min	minimum
$prob$	Probability
TD	Thermal Desorption
SB, sub	Sublimation

Greek

α	accommodation coefficients
β	Temperature exponent
θ	surface coverage
μ	Mass ratio
ν	frequency of the reaction, site exponent
ρ	number density m^{-3}
τ	characteristic time
Φ	surface site density m^{-3}
ϕ	volume fraction
χ	Scattering angle, rad
Ω	Sold angle, rad^2

Subscripts and superscripts

a	adsorbate
b	bulk
bp	bulk phase
bs	bulk species
d	desorption
eq	equilibrium
f	final, formation
g	gas-phase
i	initial, incident, incoming
int	internal
$n, norm$	normal direction
$prod$	product
$reac$	reactant, reaction
s	surface
sp	surface phase
ss	surface site set
$t, tngt$	tangential direction
tot	total

I.   Introduction

Thermal protection system (TPS) materials are used to shield space vehicles from extreme heating during hypersonic atmospheric entry missions. Important quantities like the aerothermal heating experienced by an hypersonic vehicle are directly affected by the interaction of the flow-field with the surface of the TPS. In addition, the interaction of these gases with the surface alters (both chemically and mechanically) the surface of the vehicle and modifies the chemical composition within the boundary layer. As a result, the boundary layer is far from the chemical equilibrium values, and the finite-rate nature of both the gas-phase and gas-surface reactions must be taken into account. Moreover, radiative heating predictions also depend on the concentrations of the strongly radiating surface produced species such as CN. Thus, precise knowledge of the gas-surface interactions and the chemical reactions at the surface is critical for accurate modeling of the ablation process and prediction of heat loads, leading to efficient design of the hypersonic vehicle.

In addition to chemical non-equilibirum, for many hypersonic applications, the near-surface region is not in a state of thermal equilibrium owing to the high-altitude and high-speed nature of these flows. Furthermore, commonly used TPS materials have a complicated and porous micro-structure which leads to much smaller length scales of interest at the surface. The resulting rarefaction effects make the continuum approach invalid near the surface of the vehicles. [1–4] In such a case, kinetic based methods like direct simulation Monte Carlo (DSMC), which employ a molecular description of the gas are necessary to obtain high-fidelity solutions. Although there exists a vast literature on modeling of surface chemical reactions using the continuum approach, relatively few works have examined these interactions using the DSMC method. [5–10]

Many state-of-the-art DSMC codes like SPARTA, [11] DAC, [12,13] and MAP [14] employ relatively simple surface interaction models. Surface reaction processes include only basic reaction mechanisms such as dissociation, recombination and exchange reactions. There is no provision for the gas-phase species to adsorb on the surface and undergo reactions based on finite-rate kinetics. In order to improve the surface reaction modeling capability in DSMC, a general finite-rate surface chemistry framework incorporating several reaction mechanisms is developed and implemented into SPARTA. This enables the user to model a variety of surface reactions via user-specified reaction rates and surface properties, without the need for modifying the source code. The basic approach is to stochastically model the various competing surface reaction mechanisms occurring on a set of active sites on a Langmuirian surface. Both gas-surface (GS) and pure-surface (PS) reaction mechanisms are incorporated into this framework.

This paper provides an outline of the detailed surface chemistry framework in DSMC. We also introduce new model forms for the surface reaction probabilities based on the mechanisms included in this framework. Sec.II., presents the system definitions within the proposed framework, followed by some theory and description about the various surface reaction mechanisms in Sec.III. Detailed information regarding the modeling of GS reactions and PS reactions are provided in Sec.IV., and Sec.V., respectively. Sec.VI., describes the various scattering models and Sec.VII., specifies the inputs required for this framework in DSMC. Finally, conclusions are presented in Sec.VIII.

II.   System Definitions

Recently Marschall, Maclean and Driver presented a two-part paper on a general finite rate surface chemistry model for computational fluid dynamics (CFD) solver. [15,16] The general methodology introduced in their work, namely the representation of different phases and surface sites, is adopted by the current model. A brief overview of this methodology is described below.

The system under consideration is a gas/solid material interface (Fig. 1). In addition to the gas environment, two additional environments, namely the surface interface and bulk material are included in the system model. Each environment can consist of one or more "phases", which are distinct, non-interacting regions.

The surface environment is comprised of sites, where gas-phase species can adsorb and react with species from gas, surface or bulk environments. The surface is treated as a Langmuirian surface, however all the surface sites need not be similar. Each surface environment can have multiple phases. The species adsorbed on different phases cannot interact with each other. The purpose of including multiple phases is to account for the representation of composite materials, where different regions can exhibit different types of chemical reactivity. Further, each surface phase can have multiple sets of sites. These different types of surface sites are assumed to be distributed uniformly within the surface phase. Surface reactions involving species adsorbed on different type of sites within a surface phase are possible. Such a representation of sites can be very useful for modeling different types of surfaces, for example, material containing non-homogeneous surface composition such as SiO_2, SiC, etc, or for modeling homogeneous materials containing sites of different internal bondings (electronic structure and configuration) which exhibit large

American Institute of Aeronautics and Astronautics

differences in their reactivities.[17,18] Each set of sites within each surface phase is distinct and can be distinguished for the purpose of performing surface reactions. For example, a gas-phase species can be specified to adsorb only on a particular type of site and not on other types of sites within the same surface phase. The number and concentration of surface sites and surface phases can change as the material undergoes surface-altering reactions.

The bulk environment can also contain several phases, each of them occupying a specified volume fraction. The purpose is to model composite materials like porous carbon phenolic TPS. Each of the bulk phases are assumed to be distributed uniformly and the concentration of each phase is equal to its volume fraction. As surface-altering reactions occur, the total volume of the bulk phase is allowed to change.

All of the surface and bulk environments are present within each triangular surface element in DSMC as shown in Fig. 1 (b). The surface phases and site sets are distributed uniformly throughout the surface element. Within the current framework, the motion of the adsorbed atoms are not explicitly modeled, hence the particles are deleted when they undergo adsorption. The information of the adsorbates (like surface coverage, etc.) are stored within each surface elements. All the surface reactions are performed based on the concentrations within each surface element. Currently, the surface is treated as an infinite sink and source, *i.e.,* surface morphology does not change even when they undergo bulk phase removal or addition. The change in the surface morphology as the reactions progress will be taken into account as a part of the future work.
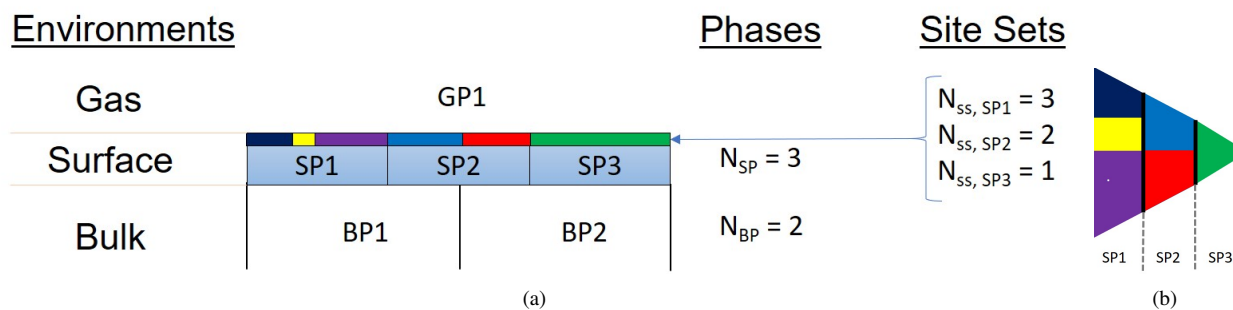

Figure 1: (a) Surface reaction framework system consisting of environments, surface phases and sets of active sites. Taken from Marschall and Maclean.[15] (b) The same framework shown within a triangular surface element in DSMC.

III.   Types of reactions

In this work, surface reactions are characterized based on the participation of the bulk-phase atoms in the reactions. If the bulk atoms only act as catalysts to promote the reaction, these are termed as catalytic reactions. On the other hand, if the bulk atoms participate in the reaction to form products, they are termed as surface participation reactions.

Surface reactions are further classified as either gas-surface (GS) or pure-surface (PS) reactions. The GS reactions involve both gas-phase and adsorbed species as reactants. On the other hand, the PS reactions involve only adsorbed (physisorbed or chemisorbed) reactants and do not include any gas-phase atoms or molecules. From a DSMC implementation viewpoint, this type of characterization based on the presence of gas-phase reactants is more meaningful since GS reactions are performed when the atom/molecules strikes the surface (as part of the *move* kernel), while PS reactions are performed separately within each time step. Hence the modeling of the GS and PS reactions will be discussed individually.

Before proceeding to the implementation details regarding the different surface reaction mechanisms, some theory that will be useful in the modeling of the surface reactions is presented in this section.

A.   Adsorption

An adsorbed atom/molecule on the surface can exist in a wide variety of configurations. For example, an oxygen atom adsorbing on a carbon surface can be bound as different functional groups: semiquinone, lactone, ether, carbonyl etc.[19,20] In addition, it can also immediately react upon adsorption through an adsorption-mediated reaction to form CO(s) that stays adsorbed on the surface. Hence within this framework, adsorption includes all the possible processes by which the incoming particle forms a bond with the surface. In order to obtain information regarding the nature of the bond or the composition of the particle after it adsorbs, the exact adsorption-mediated reaction process must be identified.

Before the adsorbing particle can settle in a particular configuration or undergo any adsorption-mediated surface reaction, it has to reach an appropriate surface site. Both direct and indirect adsorption are considered. The direct adsorption process is one in which the particle collides with the surface and immediately bonds with the site at the

point of impact. In the indirect mode, the particle first adsorbs as a precursor (intermediate). This precursor is weakly bound (maybe physisorbed) and can move freely over the surface. After a short time, it forms a bond with an appropriate adsorption site (chemisorption).
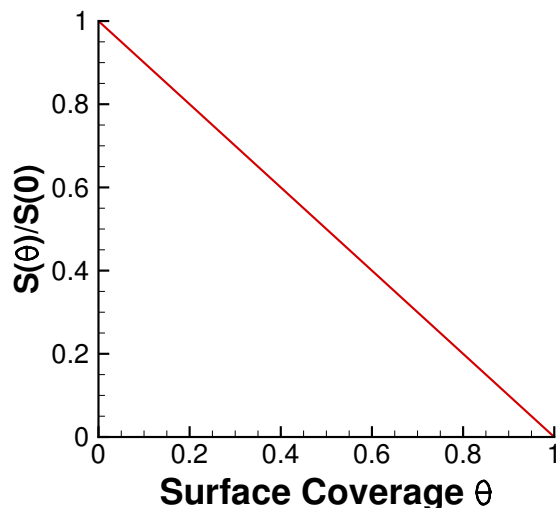
1.   Direct adsorption - Langmuir Model

Figure 2: Variation of S(θ)/S(0) with surface coverage in a Langmuir (direct) adsorption model for a single adsorbate ($\alpha = 1$).

Langmuir first proposed this direct adsorption model,[21] where the atom/molecule becomes completely immobilized upon striking the surface. In this case, the probability of adsorption depends on two factors. First, the particle must strike an empty site (not occupied by another adsorbed species), and second, this interaction with the empty site must result in an adsorption process. The probability of striking an empty site is determined based on the current surface coverage, and the probability of adsorbing on an empty site is determined by the sticking coefficient (S_0):

$$P_{ads} = S_0 * (1 - \theta)^{\alpha} \tag{1}$$

θ is the total surface coverage and S_0 is the sticking coefficient at zero surface coverage. α is the number of species that adsorb, which is 1 for associative adsorption and 2 or more for dissociative adsorption. The adsorption probability shows a linear dependence on the surface coverage. This is shown in Fig. 2 for a single adsorbate ($\alpha = 1$).
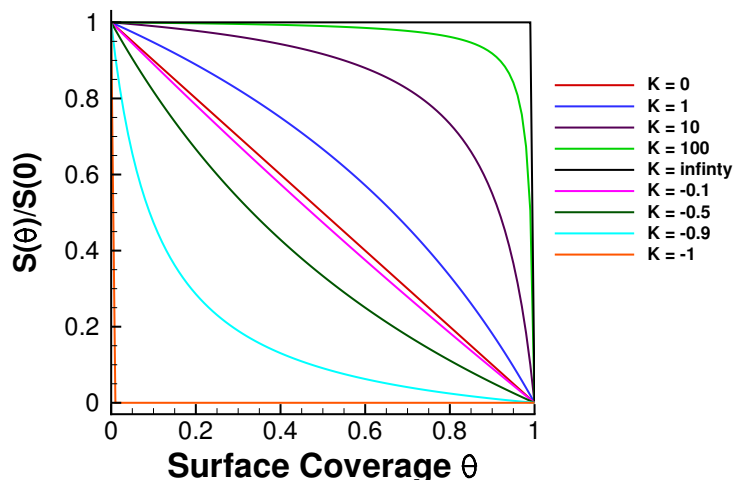
2.   Indirect adsorption - Kisliuk Model

Figure 3: Variation of S(θ)/S(0) with surface coverage according to Kisliuk's model[22] in a indirect adsorption mechanism for a single adsorbate ($\alpha = 1$).

American Institute of Aeronautics and Astronautics

In the indirect adsorption model, the particle does not chemisorb directly on the site that it first strikes. Instead, the particle gets trapped and forms a loosely bound intermediate or precursor that is short lived. This intermediate can move freely on the surface like a two-dimensional gas. If a suitable site is encountered, chemisorption of the precursor occurs, else it desorbs from the surface. A simple model for this was presented in the work of Kisliuk[22,23], where the variation of the sticking coefficient as a function of θ is modeled as:

$$\frac{S(\theta)}{S(0)} = \frac{(1 + K_{eq})(1 - \theta)^{\alpha}}{1 + K_{eq}(1 - \theta)^{\alpha}} \tag{2}$$

Here, K_{eq} is the equilibrium constant of the adsorption-desorption process of the intermediate.

$$K_{eq} = \frac{k_{ads}^*}{k_{des}^*} \tag{3}$$

Note that the notations followed here are from Somorjai.[24] The variation of sticking coefficient with surface coverage for different value of K are shown in Fig. 3. For an ideal precursor (K = ∞), the sticking coefficient is equal to S(0) for all values of θ except 1. This model reduces to the Langmuir model when K = 0. However, K is expected to have a temperature dependence. Although this model is not derived from first principles, it is well grounded in physics and reproduces many experimental observations.[22,23,25–27]

In general, the indirect or precursor-mediated adsorption is much more likely than direct adsorption. This due to the lower entropy loss encountered in the case of indirect adsorption compared to the direct adsorption.[21,24]

B. Desorption

Similar to adsorption, desorption can also occur via direct and indirect modes. Although the gas-phase products are expected to be in full thermal accommodation to the surface temperature, it is possible for some processors to alter the velocity distribution of the desorbing particles.

1. Desorption pathway

In the direct pathway, the chemisorbed particle directly desorbs into the gas-phase. The rate of the reaction will be proportional to the coverage for the direct mode.

$$r_{des} = k_{des}\theta \tag{4}$$

However, this process can also occur indirectly through a short lived precursor. In this case, the rate of desorption might not be a linear function of coverage.[24,27]

$$r_{des} = \frac{k_{des}\theta}{K_{eq}(1 - \theta) + 1} \tag{5}$$

Here K_{eq} is the equilibrium constant of the adsorption of the intermediate back to the chemisorbed state and the desorption of the intermediate into gas phase.

$$K_{eq} = \frac{k_{ads}^*}{k_{des}^*} \tag{6}$$

2. Scattering of products

If there are intermediate and elementary sub-steps involved that include energy barriers, then the desorbing gas-phase particles might have an energy distribution different from that based on the surface temperature.[28] The mean energy of the desorbing particles will be greater, but only along the surface normal direction. This is because the barrier for desorption only occurs along the surface normal direction and not along the tangential directions. The energy components are thus specified according to:
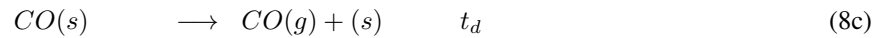
$$E_{norm} = k_b T_s + E_b \qquad E_{tngt} = k_b T_s \tag{7}$$

where k_b is the Boltzmann constant, T_s is the surface temperature and E_b is the energy of the desorption barrier. Note that this desorption barrier is different from the activation energy in the Arrhenius exponent. The activation energy describes the energy barrier of the transition state (in the rate determining step), while the desorption barrier represents the energy barrier for the last elementary step of the desorption process.

Furthermore, although the desorbing products are in thermal equilibrium with the local surface environment, they do not necessarily have energies corresponding to the bulk surface temperature. If the reaction occurs very quickly after a high energy incoming particle strikes the surface, the local surface temperature might exceed the bulk surface temperature due to the presence of local hot-spots.[29] In addition, some additional energy transfer to the products might occur as a result of dissociation or bond energy of the intermediates.

C. Langmuir-Hinshelwood (LH) mechanisms

Langmuir-Hinshelwood (LH) reaction is a pure-surface mechanism (PS), where the reaction takes place entirely on the surface and the gas-phase products are completely accommodated to the surface temperature. It has three major steps namely adsorption, formation and desorption. Since the reaction takes place on the surface, all the reactants must first adsorb on the surface sites. The second step is the formation step, where all the reactants interact on the surface to form products that are still adsorbed on the surface. Finally, the product on the surface desorbs to form gas-phase species. Each of these steps might contain many elementary sub-steps. The three steps and the final reaction for a simple CO formation on a carbon surface with adsorbed oxygen atoms is shown below.

$$O(g) + (s) \quad \longrightarrow \quad O(s) \tag{8a}$$
$$O(s) + C(b) \quad \longrightarrow \quad CO(s) \qquad\qquad t_f \tag{8b}$$
$$CO(s) \quad \longrightarrow \quad CO(g) + (s) \qquad t_d \tag{8c}$$

$$\overline{}$$

$$O(g) + C(b) \quad \longrightarrow \quad CO(g) \tag{8d}$$

In this system, $O(s)$, $CO(s)$ and $CO(g)$ are the reactant, surface intermediate, and product respectively. t_f and t_d are the characteristic times for formation and desorption respectively. Let τ be the time scale of interest, which may be the experimentally observable time scale or time scale related to other processes in the system, etc. By comparing the reaction times (t_f and t_d) and the time scale of interest τ (for instance, the rate of species diffusion in an hypersonic boundary layer), on can distinguish the following four types of LH mechanisms:

1. $t_f \ll \tau$, $t_d \ll \tau$: Prompt LH mechanism

2. $t_f \sim \tau$, $t_d \ll \tau$: LH limited by formation

3. $t_f \ll \tau$, $t_d \sim \tau$: LH limited by desorption

4. $t_f \sim \tau$, $t_d \sim \tau$: LH limited by both formation and desorption
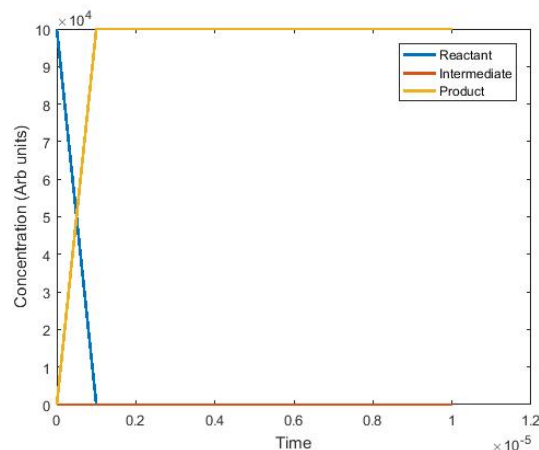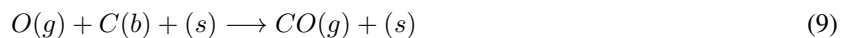
1. LH type 1

Figure 4: Concentration of the species as a function of time for a typical first-order LH reaction of type 1.

The first type of LH mechanism corresponds to a situation where both formation and desorption processes are extremely fast compared to the time scale of interest. This implies that the surface intermediate is formed immediately after the reactants strike the surface. The desorption may be a part of the formation step or an independent process that is also very quick. The variation in the concentration of all the species are shown in Fig. 4. The concentration of the reactants falls rapidly to zero in a single time step (dt = 10^{-6}). All the reactants are instantly converted to products, and the concentration of the surface intermediate remains zero. The gas-phase product exits the surface promptly at all temperatures.

For a LH mechanism of type 1 (prompt LH mechanism), both the formation and desorption processes are rapid, leading to the collapse of Eqs. (8) (b) and (c) to a single step. In DSMC, this type of LH mechanism is modeled as a

one step process with gas-phase reactants and gas-phase product. Since this reaction consists of a gas-phase reactant, it is treated as a GS reaction within DSMC (Sec.IV.).

$$O(g) + C(b) + (s) \longrightarrow CO(g) + (s) \tag{9}$$
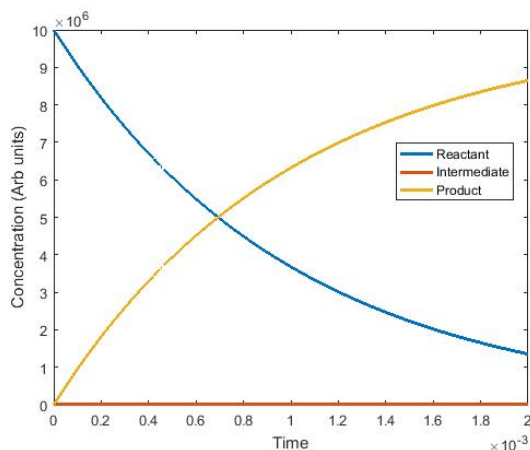
2. LH type 2

Figure 5: Concentration of the species as a function of time for a typical first-order LH reaction of type 2.

The second type of LH mechanism occurs when the time of desorption is much smaller than the time scale of interest τ, but the formation time is of the same order of τ. The formation reaction is slow and is the rate determining step (RDS) in this type of mechanism. The reactants are present on the surface for a long time before forming the surface intermediate. On the other hand, the surface intermediate forms the gas-phase products promptly since the desorption process is very rapid. Fig. 5 shows the variation in the concentration of all the species as a function of time. The concentration of the reactant decays either exponentially or based on a power law expression, depending on the order of the reaction. The product shows a corresponding increase with time, while the concentration of the intermediate remains zero.

A LH reaction system follows the characteristics of a type 2 mechanism only for a certain temperature range. If reaction rate constant of each step follows an Arrhenius form, then the time of desoprtion and formation reduces with temperature. Thus, for a fixed time scale of interest τ, a reaction system might transition from type 2 to type 1 after a certain temperature threshold.

For a type 2 LH mechanism (LH limited by formation), only the desorption step is quick, resulting in the collapse of Eq. (8) (c) into Eq. (8) (b) and giving rise to a two-step LH mechanism. This is similar to the form of LH mechanism used by Marschall and Maclean.[15] In DSMC, the first step (adsorption) is a GS reaction, while the second step is a PS reaction.

$$
\begin{aligned}
O(g) + (s) &\longrightarrow O(s) & \text{(10a)} \\
O(s) + C(b) &\longrightarrow CO(g) + (s) & \text{(10b)}
\end{aligned}
$$

3. LH type 3

The third type of LH mechanism corresponds to a situation where the formation process is rapid, and the desorption time is on the same order of the time scale of interest τ. Since the formation time is very small, the surface intermediate is formed almost instantly after the reactants strike the surface. The desorption is slow and the RDS in this type of LH mechanism. The intermediates that are formed stay at the surface for a long time before desorbing into the gas phase. The variation in the concentration of all the species are shown in Fig. 6. The concentration of the reactant falls rapidly to zero in a single time step to form the surface intermediate. The concentration of the intermediate decays (either exponential or power law based on the order of the reaction) with time, and the product concentration shows a corresponding increase. As mentioned previously, a LH reaction system might transition from type 3 to type 1 after a certain temperature threshold.

In the case of a type 3 LH mechanism (LH limited by desorption), the formation step is quick, leading to the collapse of Eq. (8) (b) into Eq. (8) (a) and giving rise to a two-step LH mechanism again. This form of a two-step LH mechanism is, however, different from the one used by Marschall and Maclean.[15] The first step is a combination of

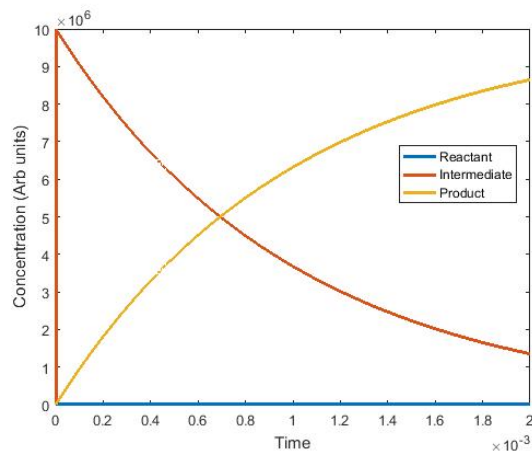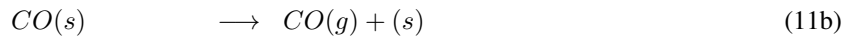American Institute of Aeronautics and Astronautics

Figure 6: Concentration of the species as a function of time for a typical first-order LH reaction of type 3.

adsorption and formation. In DSMC, this is modeled as a GS reaction (Sec.IV.), while the second step is modeled as a PS reaction (Sec.V.).

$$O(g) + (s) + C(b) \longrightarrow \quad CO(s) \tag{11a}$$
$$CO(s) \qquad\qquad \longrightarrow \quad CO(g) + (s) \tag{11b}$$
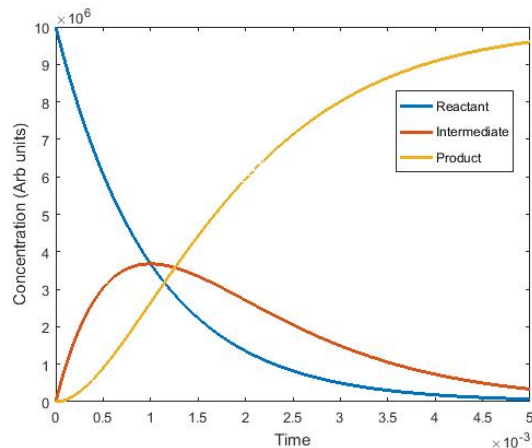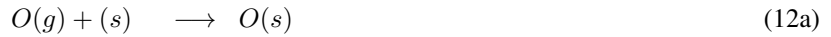
4. LH type 4

Figure 7: Concentration of the species as a function of time for a typical first-order LH reaction of type 4.

The fourth and the final type of LH mechanism occurs when both the desorption and formation times are on the order of the time scale of interest τ. Either of these reactions could be the RDS. Since there is no rapid process involved, the variation of the concentration of the reactant, intermediate and products are more complex. Fig. 7 shows the concentration of the species for a typical type 4 LH mechanism. Although the exact shape of the curves will vary widely depending on the exact values of the individual rates of formation and desorption, the same general trends are observed. The reactant concentration decreases steadily based on the rate of formation. The concentration of the intermediate shows an initial increase, where the rate of formation is greater than the rate of desorption, owing to the greater concentration of reactant compared to the intermediate. As time progresses, concentration of the intermediate reaches a peak and then starts to decrease. This results from the declining formation rate (lower concentration of reactant) and increasing desorption rate (higher concentration of intermediate). The product concentration shows a monotonic increase with time, however its rate varies widely. Initially the rate is small, which increases with time to reach a peak and then starts to fall again, following the trend of concentration of the intermediate.

For a LH mechanism of type 4 (LH limited by both formation and desorption), none of the processes are rapid, hence no simplifications can be made and no steps can be collapsed. This type of reaction must be modeled as a full three-step process. The first step, adsorption, is a GS reaction and the following two steps of formation and desorption

American Institute of Aeronautics and Astronautics

are both PS reactions.

$$O(g) + (s) \quad \longrightarrow \quad O(s) \tag{12a}$$
$$O(s) + C(b) \quad \longrightarrow \quad CO(s) \tag{12b}$$
$$CO(s) \quad \quad \longrightarrow \quad CO(g) + (s) \tag{12c}$$

D. List of Gas-Surface (GS) Reactions

From the discussion above, the different types of GS reactions include adsorption (associative and dissociative), LH mechanisms of type 1 and 3. Although LH mechanisms are PS mechanisms, the formation (and in some cases desorption) step(s) within these types of LH mechanisms occur rapidly and are modeled together with the adsorption step. The reason for not modeling all types of LH reactions as 3 steps (adsorption, formation and desorption) is that few of these involve some rapid processes. Accurately modeling these rapid processes within DSMC would needlessly place a restriction on the time step of the simulation. Thus whenever rapid sub-processes are present, they are not modeled as a separate step.

In addition to these mechanisms, other common GS reactions include condensation and Eley-Rideal (ER) mechanisms. Condensation reaction occurs when the gas-phase products adsorb on the surface and become a part of the bulk-phase material. ER mechanism is a direct impact mechanism where a gas-phase reactants directly reacts with surface (or bulk) species to form gas-phase products. Table 1 presents the list of gas-surface (GS) reactions along with examples, which are included within this framework.

Table 1: List of gas-surface (GS) reactions along with examples.

Symbol	Reaction type	Examples
1: AA	Associative Adsorption	$O(g) + (s) \longrightarrow O(s)$ $O_2(g) + (s) \longrightarrow O_2(s)$
2: DA	Dissociative Adsorption	$O_2(g) + (s) \longrightarrow O(s) + O(g)$ $O_2(g) + 2(s) \longrightarrow 2O(s)$
3: LH1	Langmuir-Hinshelwood type 1	$O(g) + (s) + O(s) \longrightarrow O_2(g) + 2(s)$ $O(g) + (s) + C(b) \longrightarrow CO(g) + (s)$
4: LH3	Langmuir-Hinshelwood type 3	$O(g) + (s) + O(s) \longrightarrow O_2(s) + 2(s)$ $O(g) + (s) + C(b) \longrightarrow CO(s) + (s)$
5: CD	Condensation	$C_3(g) + 3(s) \longrightarrow 3C(b) + 3(s)$
6: ER	Eley-Rideal	$CO(g) + O(s) \longrightarrow CO_2(g) + (s)$

E. List of Pure-Surface (PS) Reactions

The PS reactions that has been discussed so far include desorption, LH mechanisms of type 2 and 4. An additional common PS reaction is the sublimation reaction, the opposite of condensation reaction, where the bulk species sublimates into the gas-phase. Table 2 presents the list of pure-surface (PS) reactions along with examples, that is included within this framework.

Table 2: List of pure-surface (PS) reactions along with examples.

Symbol	Reaction type	Examples
1: DES	Desorption	$O(s) \longrightarrow O(g) + (s)$ $O_2(s) \longrightarrow O_2(g) + (s)$
2: LH2	Langmuir-Hinshelwood type 2	$N(s) + O(s) \longrightarrow NO(g) + 2(s)$ $O(s) + C(b) \longrightarrow CO(g) + (s)$
3: LH4	Langmuir-Hinshelwood type 4	$N(s) + O(s) \longrightarrow NO(s) + (s)$ $O(s) + C(b) \longrightarrow CO(s) + (s)$
4: SB	Sublimation	$3C(b) + 3(s) \longrightarrow C_3(g) + 3(s)$

IV. Modeling of Gas-Surface (GS) Reactions in DSMC

The GS reactions in DSMC is performed by computing the probability of a reaction when a particle strikes the surface. Thus these GS reactions are performed as a part of the *move* kernel within te DSMC structure. This section presents detailed information about modeling GS reactions in DSMC. This includes calculations of reaction probability from macroscopic rate constants and surface properties, physically consistent multi-step method for modeling multiple GS reactions without bias.

A. Adsorption

As described previously, there are different pathways through which the particle adsorbs on a surface. The probability of adsorption varies widely based on the exact pathway. However, the model provided by Kisliuk[22,23] accounts for most of these pathways by varying the equilibrium constant (K_{eq}) for the adsorption of the intermediate. The Langmuir model can also be obtained as a special case within Kisliuk's model. Hence, only this model is implemented with K_{eq} as a variable parameter.

$$P_{ads} = S^{\alpha}(\theta) \tag{13}$$

where the sticking coefficient $S^{\alpha}(\theta)$ is calculated using the following equation.

$$\frac{S^{\alpha}(\theta)}{S(0)} = \frac{(1 + K_{eq})(1 - \theta)^{\alpha}}{1 + K_{eq}(1 - \theta)^{\alpha}} \tag{14}$$

The input parameters for adsorption are the sticking coefficient at zero surface coverage (S_0) and the equilibrium constant for the adsorption of the intermediate (K_{eq}). These adsorption probability parameters are specified for each species and surface site for which adsorption reactions need to be considered.

This adsorption probability includes all the possible processes by which the incoming particle forms a bond with the surface. This does not provide information regarding the nature of the bond or the composition of the particle after it adsorbs. In order to obtain this information, the exact adsorption-mediated reaction process must be identified.

Since the explicit motion of the adsorbed atoms are modeled within this framwork, the particles are deleted when they adsorb on the surface. Only the information (such as the surface coverage, etc.) are stored within the surface elements.

B. Adsorption-mediated GS reactions

Adsorption-mediated reactions are those that involve adsorption as the first step in the reaction mechanism, for example, associative and dissociative adsorption; LH mechanisms of type 1 and 3; and condensation. Hence the probability of these reactions is calculated as the product of the reaction probability and adoption probability.

$$P_{tot} = P_{ads} * P_{reac} \tag{15}$$

1. Associative Adsorption

The probability for the associative adsorption of species A (shown below) is directly determined by:

$$A + (s) \longrightarrow A(s), \tag{16}$$

$$P_{AA} = P_{ads} * k_{AA} \tag{17}$$

where P_{ads} is the adsorption probability of A species, and k_{AA} is the rate constant for the associative adsorption reaction.

Hence, the only input parameters for an associative adsorption reaction is the rate constant k_{AA}.

2. Dissociative Adsorption

The dissociative adsorption reaction is slightly more complicated as it can involve multiple adsorbing species and also multiple gas-phase products. A general dissociative adsorption reaction can be represented by:

$$A(g) + \alpha(s) = \underbrace{B1(s) + B2(s)...}_{\alpha \text{ adsorbing products}} + \underbrace{C1(g) + C2(g)...}_{\beta \text{ gas-phase products}}$$
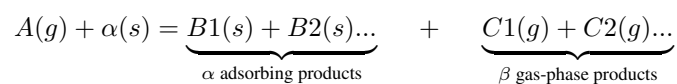
The probability of the adsorption for this case is given by:

$$P_{DA} = P_{ads} * k_{DA} \tag{18}$$

where k_{DA} is the rate constant for the dissociative adsorption reaction. The gas-phase products might become thermally accommodated to the surface temperature or still maintain the characteristics of the incoming energy. Hence the Cercignani-Lampi-Lord (CLL) model [30,31] can be used to obtain the outgoing velocities of the gas-phase products. However, there is a flexibility to use any of the scattering models available. Hence for dissociative adsorption, in addition to the rate constant, the scattering model parameters for the scattered gas-phase species must also be specified (k_{DA} + β scattering model parameters). The case where β is zero represents a situation where there is no gas-phase species and all the dissociated species adsorb on the surface.

3. LH type 1

A LH mechanism of type 1 involves gas-phase reactants and gas-phase products. A representative second-order LH type 1 reaction is shown below.

$$A(g) + (s) + B(s) \longrightarrow AB(g) + 2(s) \tag{19}$$
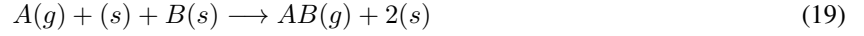
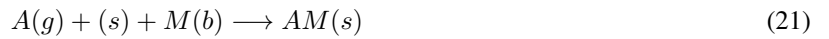The probability of this reaction is calculated as:

$$P_{LH1} = P_{ads}(A) * k_{LH1} * \frac{N_{B_s} F_N}{S_p} \tag{20}$$

Here N_{B_S} is the number of adsorbed B (DSMC) particles on the surface, F_N is the number of real particles represented by one DSMC particle, S_p is the surface area. $P_{ads}(A)$ is the adsorption probability of A species, and k_{LH1} is the rate constant for the LH type 1 reaction.

Products formed through the LH-1 mechanism are in thermal equilibrium with their surface environment and desorb based on a MB distribution at local surface temperature. However, the energy of the local surface environment might be greater than the normal surface temperature due to the formation of local hot-spots. [29,32,33] Additional energy transfer to the desorbing products might occur due to the bond energy of the intermediates or products. The angular distribution of the products follows a cosine law. In addition, both the VDF and the angular distribution of the products are altered if a desorption energy barrier is present. The thermal desorption scattering model described in Sec.VI.B. can be adequately used to account for all the above mentioned features. This however is only the recommended model and any other scattering model can instead be specified if necessary.

4. LH type 3

Modeling of LH type 3 mechanism is simpler since all the products are adsorbed species. A representative first-order LH type 3 reaction involving bulk-species is shown below.

$$A(g) + (s) + M(b) \longrightarrow AM(s) \tag{21}$$

The probability of this reaction is computed in a similar manner:

$$P_{LH3} = P_{ads}(A) * k_{LH3} \tag{22}$$

k_{LH1} is the rate constant for the LH type 3 reaction. Since the concentration of the bulk-species is treated as unity, it does not enter into the calculation of reaction probability.

Since the products remain adsorbed on the surface and do not desorb immediately, they will attain thermal accommodation with the equilibrium surface temperature. The desorption of these products are handled via the desorption reaction (Sec.V.A.1.). Hence, for LH type 3 mechanism only the rate constant of the reaction is specified.

5. Condensation

The condensation reaction is very similar to the LH type 3 mechanism, except that the products are bulk-phase, instead of surface species. The calculation of the probability is also very similar.

$$M(g) + (s) \longrightarrow M(b) + (s) \tag{23}$$

$$P_{cond} = P_{ads}(M) * k_{cond} \tag{24}$$

Unlike the LH mechanisms, the adsorption of species is not listed as a separate reaction. Hence, the equilibrium constant (of the intermediates) from the Kisliuk's model should also be specified in addition to the rate of the reaction.

C. Direct Impact GS reactions

Direct Impact (DI) mechanisms occur immediately after the gas-phase reactant strikes the surface. They do not involve adsorption as the initial step.

1. Eley-Rideal (ER) Mechanism

An ER reaction is an impulsive surface mechanism, where a gas-phase atom/molecule directly interacts with a reactant present on the surface to form gaseous products. The reaction kinetics of this mechanism are dependent upon both the surface and gas-phase reactant:

$$A(g) + B(s) \longrightarrow AB + (s). \tag{25}$$

The probability P_{ER} of the impact of particle A resulting in an ER reaction was derived by Molchanova *et al.,* [10] as

$$P_{ER} = 2k_{ER}\frac{N_{B(s)}F_N}{S_p}\frac{1}{v_n}. \tag{26}$$

Here, v_n is the velocity of the impacting particle along the surface normal. It should be noted, however, that the rate constant k_{ER} is based on the surface temperature and not on the gas temperature. This is because using the latter yielded unphysical results. [10]

The ER mechanism is by definition a non-thermal mechanism, whereby the energy distribution of the products do not follow a MB distribution based on the surface temperature, but are instead characterized by the incident particle energy. This is due to the fact that the products of the ER mechanism are formed immediately after the gas-phase reactant strikes the surface and the interaction time is not long enough for thermal equilibration with the surface. The products have translational energies that are significantly higher than the MB distribution based on the surface temperature. The angular distributions of the ER products do not follow a particular distribution and are reported in the literature to vary depending on the reaction. The only consistent feature is that a peak in angular distributions occurs on the opposite side of the surface normal from the incident beam. The scattering of the ER products can be described using a non-thermal scattering model (Sec.VI.D.).

D. Performing GS reactions without bias

The GS reactions are performed in DSMC by specifying a probability. Since the probabilities are calculated from the rates, the individual or the cumulative probability of all the various possible reactions might be greater than unity. In such cases, determining the probabilities of the GS reactions in a physically consistent manner is very important in order to avoid any bias. In this regard, the following sequence of steps is proposed.

1. First the probability of total adsoprtion is calculated from the Kisliuk's model, given by

$$P_{ads} = (1 - S_\theta) \qquad S(\theta) = S(0)\left(1 + \frac{\theta}{1-\theta}K\right)^{-1} \tag{27}$$

   where K is the equilibrium constant of the adsorption-desorption process of the intermediate. Note that this represents the total probability of adsorption, not of any particular adsorption-mediated GS reactions.

2. Next, the probability of direct impact mechanisms are computed as specified in Sec.IV.C.

3. Now, the probability of scattering without undergoing any reaction is calculated.

$$P_{scatter} = \begin{cases} 0, & \text{if } P_{ads} + sum(P_{DI}) > 1. \\ 1 - (P_{ads} + sum(P_{DI})), & \text{otherwise.} \end{cases} \tag{28}$$

   $sum(P_{DI})$ represents the total probability of all the direct impact (DI) mechanisms. If the sum of the reaction probabilities (total adsorption and direct impact mechanisms) is less than 1, then the probability of scattering is calculated in a straightforward manner. However, if the sum of the reaction probabilities exceeds 1, then the scattering probability becomes zero. Also, the probabilities must be normalized to ensure that we do not introduce any bias towards the initial reactions (Appendix A). The normalization is straightforward: each reaction probability is divided by $P_{ads} + sum(P_{DI})$.

4. Finally, we compute the probabilities of the adsorption-mediated (AM) GS reactions. The initial probabilities of these reactions are computed as presented in Sec.IV.B. It is highly unlikely that these probabilities will exactly add up to the adsorption probability P_{ads}. Hence another normalization is performed by dividing the adsorption-mediated reaction probabilities with the factor $sum(P_{AM})/P_{ads}$.

Note that two different normalizations are performed. The first normalization is over all the reactions (adsorption and direct-impact) and ensures that the total probability of all possible pathways sum to unity. The second normalization is performed within adsorption-mediated GS reactions since their sum must be equal to the total adsorption probability P_{ads}.

V.   Modeling of Pure-Surface (PS) Reactions in DSMC

This section presents detailed information about modeling PS reactions in DSMC. Unlike GS reactions, PS reactions cannot be modeled by specifying a probability value. A PS reaction is performed by determining the time between two consecutive events.[10] For a process P, with frequency ν_P, the characteristic time, which is defined as the time between two consecutive events of P, can be calculated as:

$$t_P = -\frac{ln(Rn)}{\nu_P} \tag{29}$$

where Rn is a uniform random number in (0,1]. This section presents the methods to obtain the characteristic frequencies of the various reactions and provides the details on how to model multiple PS reactions without bias. These PS reactions are performed within each time step by looping over all the surface elements. This can be performed in parallel with the collisions in the gas-phase.

A.   Computing Characteristic Frequency

1.   Desorption

In order to model desorption reaction, the time between two desorption reactions is computed from the reaction rate constant of the desorption process.

$$A(s) \longrightarrow A + (s). \tag{30}$$

If the rate of this desorption reaction is given by:

$$\frac{dn_{A(s)}}{dt} = -k_{des}n_{A(s)}, \tag{31}$$

where k_{des} is the desorption reaction rate constant and $n_{A(s)}$ is the surface number density of the adsorbed species $A(s)$. Although here it is assumed that the rate of desorption is linearly proportional to the surface coverage, this might not always be the case (Sec.III.B.). The characteristic frequency of this desorption process is

$$\nu_{des} = k_{des}N_{A(s)}. \tag{32}$$

The time through which the particle remains on the surface before desorption may be calculated using the characteristic frequency[10]:

$$\tau_{des} = -\frac{log(Rn)}{\nu_{des}}, \tag{33}$$

where Rn is a uniform random number in (0,1]. The desorption reaction is performed using the time counter algorithms based on the current value of the frequency and characteristic times. For a desorption mechanism, the rate constant k_{des} and the scattering model parameters for the desorbing products must be given as input.

Desorption is a thermal mechanism and the products exit based on a MB distribution at the local surface temperature. In some cases, it is possible that the local surface environment has energies greater than the bulk surface temperature due to the presence of local hot-spots. Further, additional energy transfer to the products might occur from the dissociation or bonding energy of the intermediate/products. This would alter the final VDF of the desorbing products, while the angular distribution is not affected.

Furthermore, the desorption of the surface species might have an energy barrier associated with it. This is the energy the adsorbed atom/molecule needs to overcome in order to escape from the surface. This may be the bonding energy of the species or some intermediate. Usually this desorption barrier exists only along the surface normal direction. Thus, the presence of a barrier will alter both the VDF and angular distribution of the desorbing species. The computational modeling of thermal desorption in the presence of local hot-spots, additional energy transfer and desorption energy barrier and their effect on the final distribution is presented in more detail in the thermal desorption model (Sec.VI.B.).

2. LH type 2

In a LH surface reaction mechanism, all the reactants adsorb on nearby surface sites. They then undergo reaction that form products desorbing into the gas phase. For a LH reaction involving two distinct reactants A and B of the form:

$$A(s) + B(s) \longrightarrow AB(g) + 2(s). \tag{34}$$

The reaction rate for the above reaction is given by:

$$\frac{dn_{A(s)}}{dt} = \frac{dn_{B(s)}}{dt} = -k_{LH} n_{A(s)} n_{B(s)}. \tag{35}$$

Similar to the case of desorption, the frequency of the LH reaction can be calculated as:

$$\nu_{LH} = k_{LH} N_{A(s)} N_{B(s)} \frac{F_N}{S_p}, \tag{36}$$

where S_p is the area of the surface element and F_N is the number of real particles represented by one simulated particle in DSMC. The frequency for the LH recombination reactions between the same reactant species, described by the mechanism:

$$A(s) + A(s) \longrightarrow A_2(g) + 2(s), \tag{37}$$

can be shown to be[10]:

$$\nu_{LH} = k_{LH} \frac{N_{A(s)} \left(N_{A(s)} - 1\right)}{2} \frac{F_N}{S_p}. \tag{38}$$

LH surface reactions that involve a bulk species as one of the reactants, become pseudo first-order since the concentration of the bulk species is treated as unity:

$$A(s) + M(b) \longrightarrow AM(g) + (s). \tag{39}$$

For such reactions, the characteristic frequency can be derived as:

$$\nu_{LH} = k_{LH} N_{A(s)}. \tag{40}$$

Finally, the characteristic time between two LH reactions (for all types) is given by:

$$\tau_{LH} = -\frac{log(Rn)}{\nu_{LH}}. \tag{41}$$

Hence, for a LH type 2 reaction the rate constant k_{LH2} and the desorption barrier E_b should be specified. The flux PDF and angular distribution of the products for a LH type 2 reaction desorb based on the surface temperature and the desorption barrier of the particular species, similar to the desorption reaction.

3. LH type 4

Modeling of LH type 4 mechanism is easier since the products are adsorbed species. Representative reactions for LH type 4 mechanism are shown below.

$$A(s) + B(s) \longrightarrow AB(s) + (s) \tag{42a}$$
$$A(s) + A(s) \longrightarrow A_2(s) + (s) \tag{42b}$$
$$A(s) + M(b) \longrightarrow AM(s) \tag{42c}$$

The characteristic frequencies and times are calculated similar to LH type 2 mechanism. Only the rate constant for the reaction k_{LH4} needs to be specified.

4. Sublimation

The sublimation reaction is very similar to LH type 2 reaction, except that the reactants are bulk-phase species, instead of adsorbed species.

$$(s) + M(b) \longrightarrow M(g) + (s) \tag{43}$$

The formula for computing the characteristic times and frequencies remain the same, however, they will now be based on the available empty sites, rather than on filled sites. Since this reaction involves a gas-phase product, the scattering model for that species should be specified in addition to the rate constant k_{sub}.

B.   Time-counter algorithm for modeling PS reactions

1.   Basic time counter algorithm

For modeling other PS reactions in DSMC, a time counter method is used. The PS reactions that occur on the surface element during the time step Δt are consecutively performed at the end of each time step. For a single PS reaction, the following iterative process is used.[10]


Algorithm 1 Simple Molchanova

1: **procedure** PS REACTIONS
2:       $\tau_{LH} = \tau_{LH} + dt$
3:       **while** $\tau_{LH} > 0$ **do**
4:              Perform the reaction
5:              $\tau_{LH} \leftarrow \tau_{LH} - t_{LH}$
6:              update ν_{LH}
7:              $t_{LH} = \frac{-ln(Rn)}{\nu_{LH}}$

τ_{LH} is the time counter that is used to perform the simulations. ν_{LH} is updated after every reaction owing to the change in the concentration of the reactants, and a new value for t_{LH} is computed. Note that this process is correct only in the case of a single reaction. The algorithms for accurately modeling multiple PS reactions (using the time counter method) without bias is described in detail in Sec.V.C.

2.   Extension to multiple reactions

The approach described in the previous section was verified to reproduce the theoretical (or analytical) expression for a single LH reaction.[10] However, the extension of this approach for multiple reactions is not straightforward. Using the same methodology and sequentially performing the various reactions introduces a bias towards the initial reactions.

For example, consider the following case with two possible LH reactions occurring simultaneously on a carbon surface filled with adsorbed oxygen atoms.

$$2O(s) \longrightarrow O_2(g) + 2(s)$$
$$2O(s) + C(b) \longrightarrow CO_2(g) + 2(s) \tag{44}$$
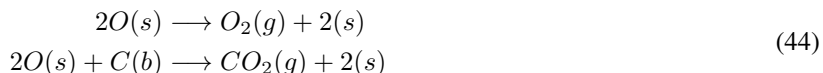
Performing the two reactions sequentially in the manner described above leads to the following result for the flux and rate for each product, shown in Fig. 8. The surface is initially filled with adsorbed oxygen, which then undergo the aforementioned LH reactions (according to the specified rate constants) to form product O_2 and CO_2. The analytical solution is also plotted alongside for comparison. In this case, the rate constants for the two reactions were set equal to each other. Since both the LH reactions are second order, we would expect the flux and rate of both the reactions to be the same, as seen from the analytical solution. However, the DSMC solution obtained using the Molchanova's approach with sequential ordering of reactions shows discrepancies in comparison with the analytical solution. The first reaction (O_2 formation) is favored over the second reaction (CO_2 formation), leading to a bias. Both these reactions lead to depletion of adsorbed O atoms, which tends to decrease the rate of both the reactions. Since all possible O_2 formation reactions within a time step are performed first, before considering the CO_2 formation reaction, the rates of O_2 reaction is consistently higher, leading to higher flux compared to CO_2. In summary, the sequential handling of multiple reactions with the Molchanova's method leads to a bias towards the reactions considered first.

In cases where the time step size of the simulation is much smaller compared to the reaction time scales, the observed bias between the multiple reactions decreases as shown in Fig. 9. This figure shows the comparison between the analytical solution and the DSMC simulations for the same case described above, but with a much smaller time step size. In this scenario, the frequency of each reaction is not high enough for a single reaction to be repeated several times within one time step. Thus, the change in concentration of adsorbed oxygen atoms due to one particular reaction is negligible compared to the total concentration. This ensures that the reaction rate is not appreciable affected by the particular sequence in which the reactions are performed and thus leads to reduction in bias. However, reducing the time step size to remove the bias is not viable solution in DSMC. In many cases, the reaction rates at the surface might be extremely high, placing a large restriction on the time step size. This leads to an unnecessary increase in the computational requirements and restricts the total run time of the simulation.

The following section describes two methods to remove the bias introduced by sequential handling of multiple reactions within Molchanova's approach.[10] The first method retains the framework of performing the reactions, while altering the order of reactions to remove the bias. The second method provides a more elegant approach of performing the reactions, similar to the one followed in kinetic Monte Carlo (kMC) simulations.[34]
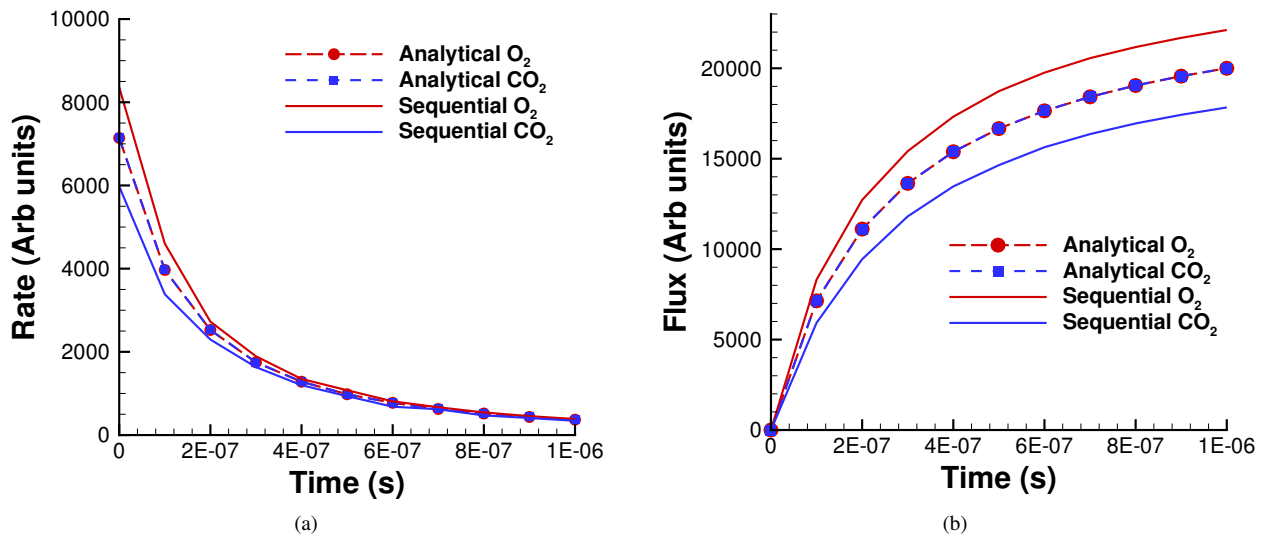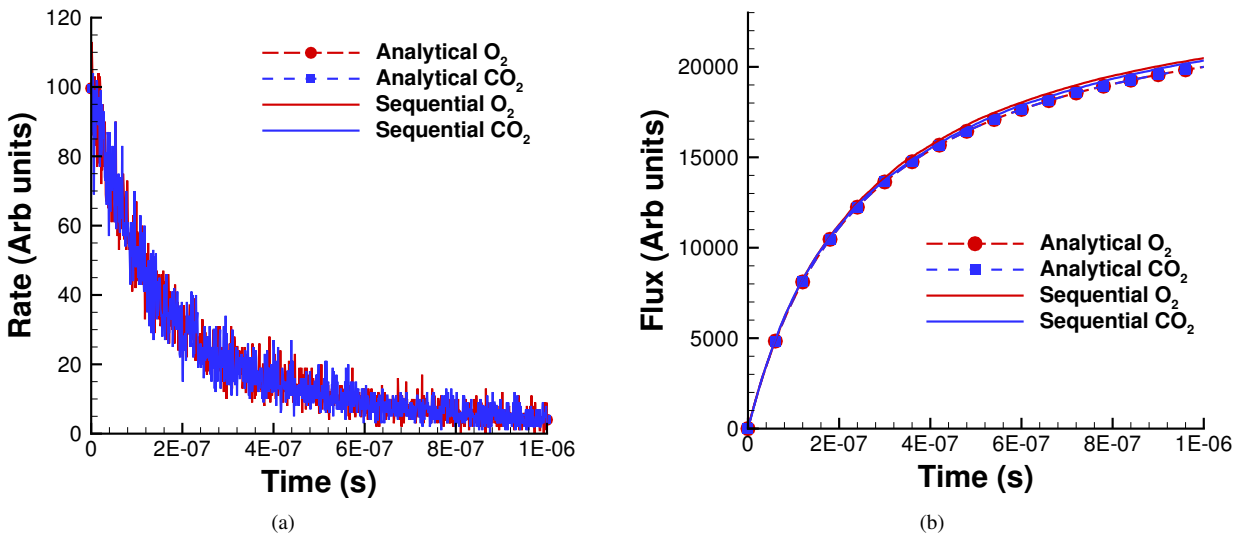

Figure 8: (a) Rate of formation and (b) total flux of products as a function of time obtained from the analytical solution and DSMC simulation using Molchanova's method with sequential handling of reactions and a relatively large time step size.

Figure 9: (a) Rate of formation and (b) total flux of products as a function of time obtained from the analytical solution and DSMC simulation using Molchanova's method with sequential handling of reactions and a relatively small time step size.

C. Time-counter algorithms without bias

1. Algorithm A

In this algorithm, the order of the various possible reactions are altered to ensure that there is no bias introduced while performing the reactions. The reactions are not performed sequentially in a pre-determined order, however are chosen based on their rates, after each reaction is performed. Higher the rate of a reaction, greater its frequency and larger probability of occurring. At any instant, the total count of a reaction within the time step is determined by the product of τ (time counter) and ν (frequency). In addition to capturing the dependence on frequency, it also reduces the probability of reaction that have already occurred within the particular time step. When a reaction is performed, the value of that particular time counter τ is decremented, thus reducing the probability of the reaction. In other words, the probability of all the reactions are adjusted such that within a single time step, the relative selectivity of each reaction
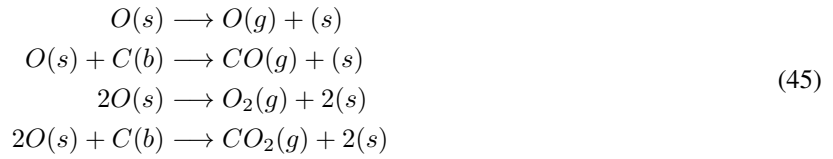
American Institute of Aeronautics and Astronautics

is exactly satisfied.[§]

Algorithm 2

1: **procedure** ALGORITHM A
2:     **for** $i \leftarrow 1$ to Number of reactions **do**
3:         $\tau_{LH}(i) = \tau_{LH}(i) + dt$
4:     $sum = 0$
5:     **while** (1) **do**
6:         **for** $i \leftarrow 1$ to Number of reactions **do**
7:             update $\nu_{LH}(i)$
8:             $t_{LH}(i) \leftarrow -\frac{ln(Rn)}{\nu_{LH}(i)}$
9:             $sum \leftarrow sum + round(\tau_{LH}(i) * \nu_{LH}(i))$
10:         **if** $sum == 0$ **then** break
11:         **for** $i \leftarrow 1$ to Number of reactions **do**
12:             $prob(i) \leftarrow \frac{round(\tau_{LH}(i)*\nu_{LH}(i))}{sum}$
13:         Choose one reaction randomly based on prob values
14:         Perform the reaction
15:         $\tau_{LH} \leftarrow \tau_{LH} - t_{LH}$

This algorithm updates the value of ν_{LH} of all the reactions after each reaction. And each reaction is chosen based on the updated value of its count ($\tau * \nu$), thus leading to a system without bias regardless of the time step size. A more complex reaction set with four possible LH reactions (shown below) of varying orders and rate constants is chosen to showcase the validity of the present approach.

$$
\begin{aligned}
O(s) &\longrightarrow O(g) + (s) \\
O(s) + C(b) &\longrightarrow CO(g) + (s) \\
2O(s) &\longrightarrow O_2(g) + 2(s) \\
2O(s) + C(b) &\longrightarrow CO_2(g) + 2(s)
\end{aligned}
\tag{45}
$$

Figs. 10 and 11 present the comparison of the analytical solution with the DSMC simulation results obtained using Algorithm A for a relatively small and large time step size respectively.
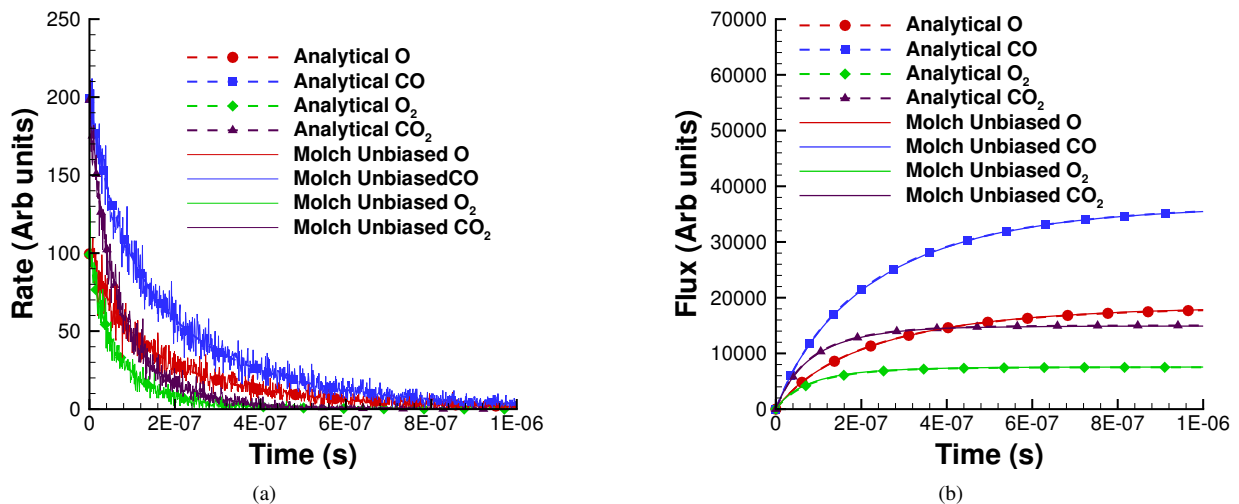

Figure 10: (a) Rate of formation and (b) total flux of products as a function of time obtained from the analytical solution and DSMC simulation using Algorithm A and a relatively small time step size.

[§]For example, lets say that the probability of 2 events A and B is both 0.5. For each set of 10 events, if the count of events A and B is exactly 5, then it is said that the relative selectivity of each event is exactly satisfied.
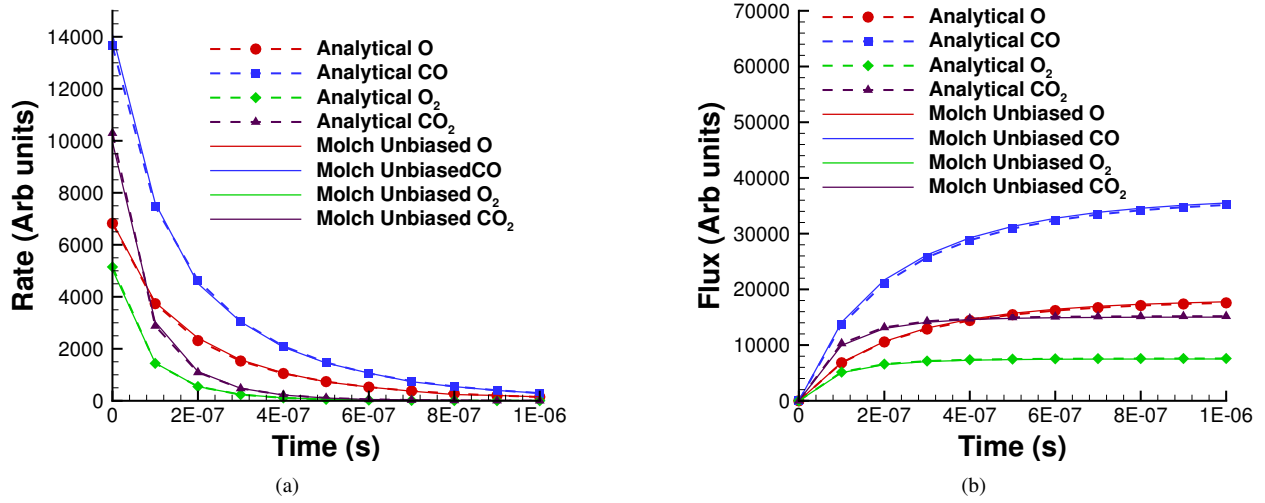
American Institute of Aeronautics and Astronautics

Figure 11: (a) Rate of formation and (b) total flux of products as a function of time obtained from the analytical solution and DSMC simulation using Algorithm A and a relatively large time step size.

2. Algorithm B

In the previous algorithm, a separate time counter was utilized for each of the reaction. Instead of this, we can use a single time counter (for each surface element) to accurately perform multiple LH reactions without bias. This algorithm closely resembles the direct method for kinetic Monte Carlo (kMC) simulations proposed by Gillespie.[34] Similar to the previous approach, the order of the reaction is not pre-determined. However, the probability of each reaction is determined based solely on the frequency of each reaction (ν), and not the count ($\tau * \nu$). This algorithm is detailed below.

Algorithm 3

1: **procedure** ALGORITHM B
2:     $\tau_{LH} = \tau_{LH} + dt$
3:     **while** $tau_{LH} > 0$ **do**
4:         $sum = 0$
5:         **for** $i \leftarrow 1$ to Number of reactions **do**
6:             update $\nu_{LH}(i)$
7:             $sum \leftarrow sum + \nu_{LH}(i)$
8:         **for** $i \leftarrow 1$ to Number of reactions **do**
9:             $prob(i) \leftarrow \frac{round(\nu_{LH}(i))}{sum}$
10:        Choose one reaction randomly based on prob values
11:        Perform the reaction
12:        $t_{LH} \leftarrow \frac{-ln(Rn)}{sum}$
13:        $\tau_{LH} \leftarrow \tau_{LH} - t_{LH}$

Note the expression for t_{LH} is based on the sum of all the reaction frequencies and remains unchanged regardless of the particular reaction that is carried out. Remember that the characteristic time between two consecutive events of a particular LH reaction is given by:

$$t_{LH}(i) = -\frac{log(Rn)}{\nu_{LH}(i)} \qquad (46)$$

Extending this, the characteristic time between any two LH reaction can be written as:

$$t_{LH} = -\frac{log(Rn)}{\sum_i \nu_{LH}(i)} \qquad (47)$$

Hence, regardless of the reaction performed, the characteristic time value is calculated in a similar manner, and is used for decrementing the common time counter. The adoption of such a combined characteristic time allows the use of a single time counter for multiple reactions (on each surface element). Since the probability of the reaction is only based

on its frequency (and not the count), the probabilities are not influenced by the number of previous occurrences of each reaction within a time step. Thus, in this algorithm, the relative selectivity of each reaction is only statistically (not exactly) satisfied.¶ Similar to the previous approach, the DSMC simulations performed using Algorithm B provides excellent agreement with the analytical solutions regardless of the time step size as shown in Figs. 12 and 13.
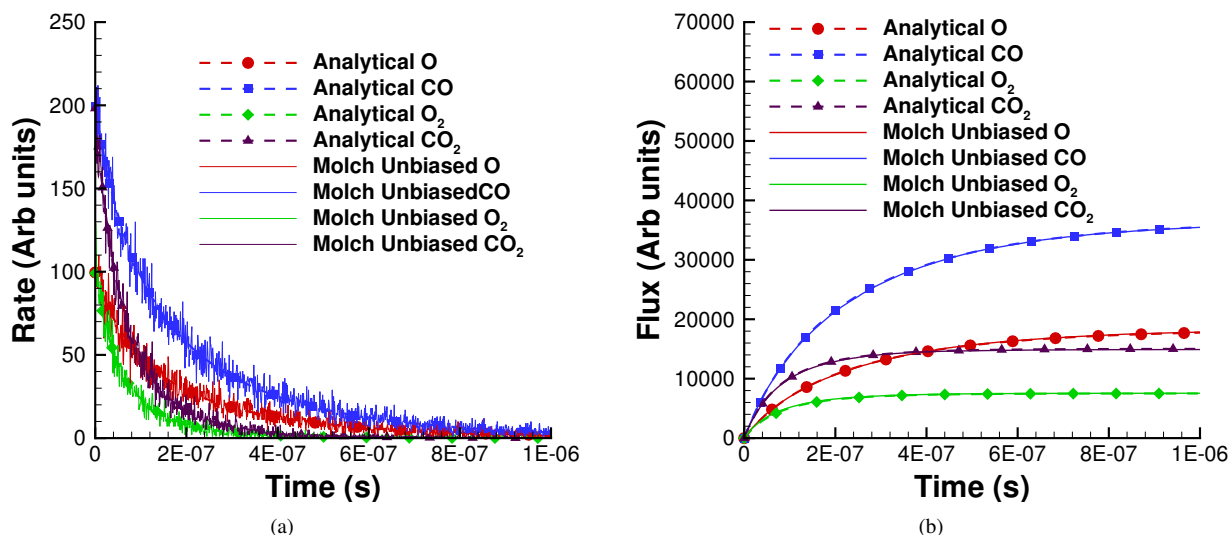

(a)

(b)

Figure 12: (a) Rate of formation and (b) total flux of products as a function of time obtained from the analytical solution and DSMC simulation using Algorithm B and a relatively small time step size.
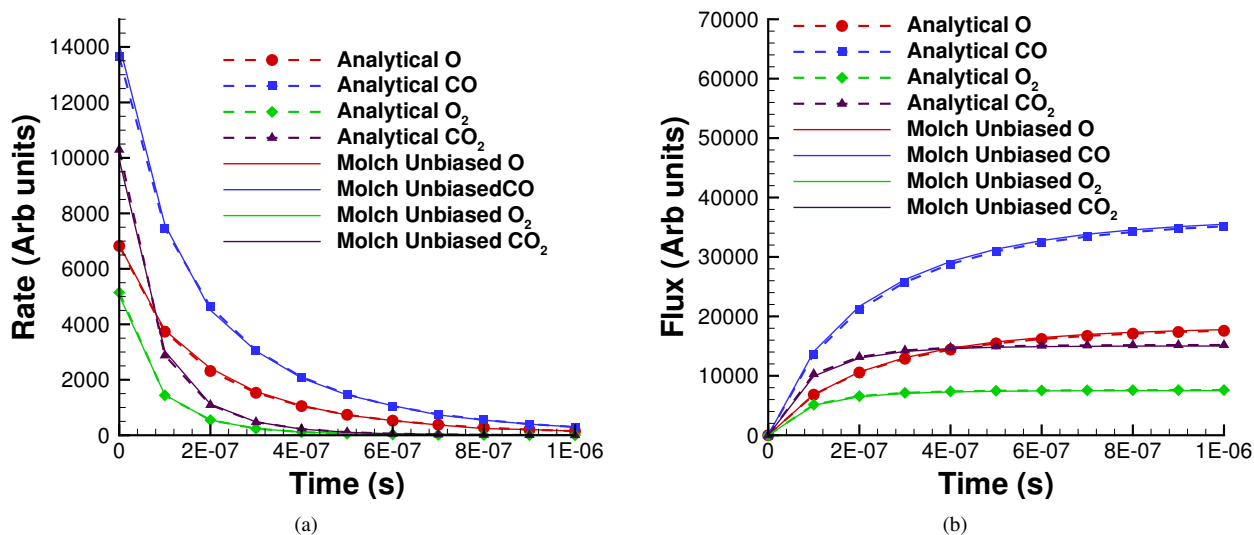

(a)

(b)

Figure 13: (a) Rate of formation and (b) total flux of products as a function of time obtained from the analytical solution and DSMC simulation using Algorithm B and a relatively large time step size.

In conclusion, the approach outlined by Molchanova *et al.,*[10] for performing LH reactions cannot be directly extended to the case of multiple reactions. It was shown that a simple sequential handling of multiple reactions can lead to a system bias towards initial reactions, depending on the time step size. In order to eliminate this bias, two algorithms were proposed. The first approach involves changing the order of the reactions while the methodology to perform the reactions remains similar to the method proposed by Molchanova *et al.*[10] The second approach is inspired by direct method of Gillespie[34] employed in kinetic Monte Carlo (kMC) simulations and alters both the order of the

_____

¶For example, lets say that the probability of 2 events A and B is both 0.5. For each set of 10 events, if the count of events A and B is not exactly 5, but on an average 5. It could be (6,4); (7,3); (4,6); (3,7), etc. If this is the case, then it is said that the relative selectivity of each event is statistically satisfied.¶

American Institute of Aeronautics and Astronautics

reactions and methodology of performing them. Both the approaches were shown to reproduce analytical results for a multi-reaction system regardless of the time step size. The first approach exactly satisfies the relative selectivity of the multiple reactions, while the second approach statistically satisfies it. Depending on the particular application and requisite statistical properties of the system, an appropriate approach can be chosen. In the absence of any preference, the second approach is recommended owing to the relatively lower memory requirements and computational cost.

VI. Scattering models in DSMC

When a particle strikes the surface, it can either adsorb, undergo a direct impact reaction, or scatter impulsively (without undergoing any reaction) from the surface. If the energy of the incoming particles is low (thermal energies, i.e., comparable to the temperature of the gas), then the scattering of the particle could be reasonably modeled using the CLL model.[30,31] However, if the particles strike the surface with super or hyper-thermal velocities, the CLL model cannot be used to predict the energy and angular distribution of the scattered products. Hence, a non-thermal and impulsive scattering models are developed and implemented in DSMC to account for the scattering of particles with super and hyper-thermal incident energies respectively. In addition, there is absence of models in DSMC to describe the scattering of the desorbed products formed on the surface. Here, a new model called the thermal desorption model is also developed and described.

A. CLL model

Of various phenomenological models for gas-surface interactions, the CLL model[30] appears to be most comprehensive. This model satisfies detailed balance (reciprocity) and produces physically reasonable velocity and angular distributions of the scattered particles. And unlike the Maxwell's model, it provides a continuous variation from specular reflection to diffuse reflection with full thermal accommodation.

In the original model, two accommodation coefficients for the normal and tangential directions (α_n, α_t) are employed. Each of these quantities can take a value between 0 and 1. Specular reflection is achieved by using the values {0,0}, while complete thermal accommodation with the surface and cosine angular distributions is obtained using {1,1}. There is smooth variation of both the energy and angular distribution for values in between these limits.

In addition to this spectrum with extreme ends, Lord[31] has proposed a way to take into account other scenarios such as fully and partially diffuse scattering with incomplete energy accommodation. This can reproduce a lobular distribution using the eccentricity factor e. Further, extension of the CLL model was also proposed to handle internal degrees of freedom, described using continuous and discrete energy levels, including anharmonic distribution.

The implementation of the CLL model within the current implementation of the CLL model takes 4 inputs for translational mode. These are the normal and surface accommodation coefficient (α_n, α_t), the accommodation coefficients for internal energies: rotational, vibrational $(\alpha_{rot}, \alpha_{vib})$. Also, there is an additional option of specifying the eccentricity parameter e. The current code is capable of handling both continuous and discrete harmonic energy levels for vibrational degrees of freedom. However the case of anharmonic discrete energy levels is not incorporated since SPARTA does not have that capability yet. The internal energy accommodation values must be specified even for an atomic species, however these values are simply ignored.

The eccentricity parameter is used to capture partially diffuse scattering, independent of the level of energy accommodation. The range of e is [0,1]. A value of 1 implies a fully diffuse scattering (with a cosine distribution), and the distribution becomes more lobular as the value decreases. Specifying 0 for the value of e implies specular scattering at the same angle of incidence, but with partial or complete energy accommodation. Any other value for the eccentricity parameter does not invoke the partially diffuse scattering model and the angular distribution is obtained based on the energy accommodation.

B. Thermal desorption model

1. Desorption energy barrier

Due to the nature of the interaction between the products and the surface, the desorption of the products might have an energy barrier. For a surface desorption process, this desorption barrier exists only in the normal direction. Thus, only the products having enough energy (in the normal direction) to overcome the barrier will be able to desorb from the surface. This alters the velocity distribution of the observed products along the surface normal direction and thus leads to the distortion of the speed distribution.[35] Fig. 14 (a) shows a representative flux PDF of a thermal process with and without a desorption barrier. In the presence of a desorption barrier, the flux PDF is shifted towards the right (shorter surface-to-detector flight times) of a MB distribution. The angular distributions, which represent the ratio of the normal to the tangential velocities, are also altered as a result of the desorption barrier. The angular distributions are peaked more towards the normal and are often described by a cosine power law distribution $(cos^n\theta)$.

In order to obtain the cosine power law distribution in DSMC, the tangential velocities of desorbing molecules must be based on the surface temperature, and the normal velocity component must be drawn from a Boltzmann
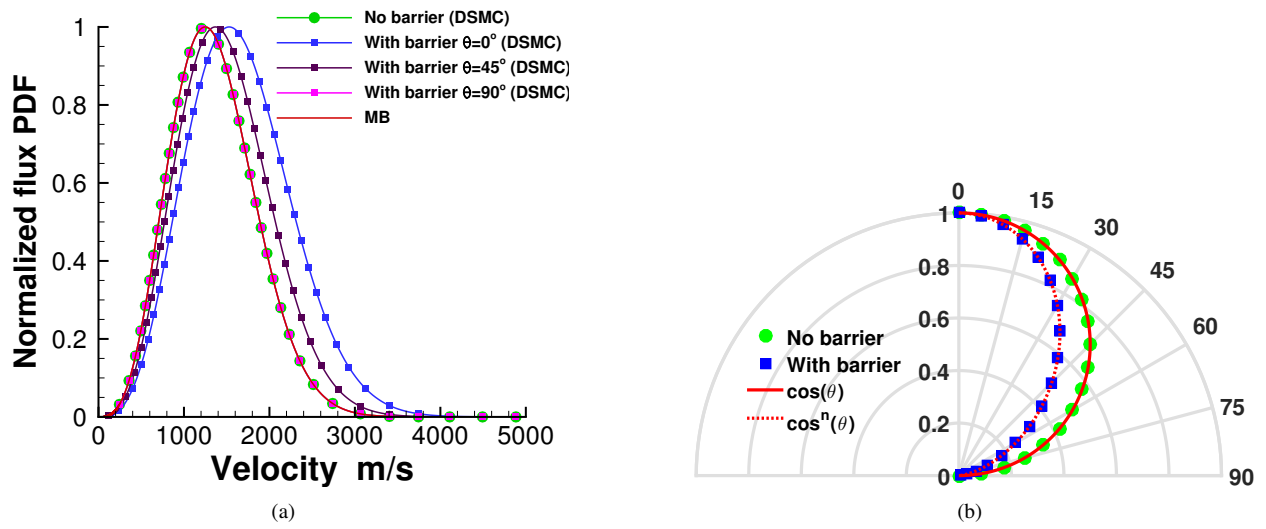
Figure 14: (a) Representative flux PDF distributions of products formed via a thermal mechanism with and without a desorption barrier from a smooth surface for a hyperthermal beam. The distributions are plotted at angle $\theta = 0°, 45°, 90°$ for the case with the desorption energy barrier. (b) Representative in-plane angular distributions of products formed via a thermal mechanism with and without a desorption barrier from a smooth surface (n = 1.5).

distribution based on a different temperature given by:

$$T_{norm} = T_s \left(1 + \frac{E_b}{k_b} \right). \tag{48}$$

The value of the desorption barrier E_b for a given cosine power law distribution ($cos^n \theta$) can be obtained as[35]:

$$E_b = \left(\frac{n-1}{2} \right) k_b T_s. \tag{49}$$

In the presence of the energy barrier, the final VDF/SDF will depend on the polar angle. The analytical form of the distribution can be computed as:

$$f(v) \propto v^2 exp \left(-\frac{mv^2}{2k_b} \left(\frac{cos^2\theta}{T_n} + \frac{sin^2\theta}{T_t} \right) \right) \tag{50}$$

C. Impulsive scattering model

When particles having super or hyper-thermal velocities strike the surface, their scattering patterns are very different from those in the thermal regime.[36] The final energy distribution of the particles exhibit dependence on the incoming energy, angle of incidence and reflection, temperature of the surface, interaction potential, etc.

1. VDF

The velocity distribution of the IS component can be reasonably approximated using a Gaussian distribution with a mean u_0 and a variance α following Rettner.[37] These two are treated as free parameters in the DSMC model that can be adjusted to match the IS component of the experimental distributions.

$$f_{IS}(u) \propto u^2 \, exp \left(-\frac{(u - u_0)^2}{2\alpha^2} \right) \tag{51}$$

2. Angular dependence of VDF parameters: Soft-sphere scattering model

The dependence of the scattered particle energy distribution on the incident energy and angle can be captured using the soft-sphere scattering model. At such high energies, the projectile interacts with the surface in the limit of atomic collisions.[36] Hence, this kinematic model is based on a treatment of soft-sphere scattering , in which a gas-phase, soft-sphere projectile, with an incidence translational energy of E_i, undergoes an inelastic collision with a soft sphere on the surface.[38] The average final energy of the particles is given by:
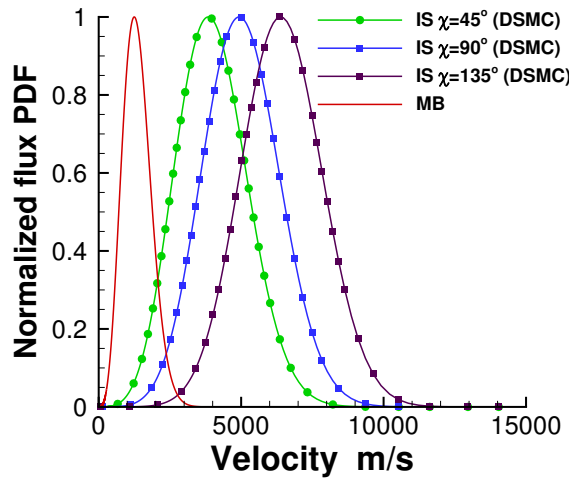
American Institute of Aeronautics and Astronautics

Figure 15: Representative flux PDF distributions of impulsively scattered (IS) atoms at deflection angles $\chi = 45°, 90°, 135°$ from a smooth surface for a hyperthermal beam.

$$\langle E_f \rangle = E_i \left(1 - \frac{2\mu}{(\mu+1)^2} \left[1 + \mu sin^2\chi + \frac{E_{int}}{E_i} \left(\frac{\mu+1}{2\mu} \right) - cos\chi \sqrt{1 - \mu^2 sin^2\chi - \frac{E_{int}}{E_i}(\mu+1)} \right] \right) \qquad (52)$$

Here, μ is the mass ratio of the gas and surface species. E_{int} is the energy transferred to the internal energy. This becomes zero in the case of hard-sphere scattering. The deflection angle χ is defined as:

$$\chi = 180^o - \theta_i - \theta_f \qquad (53)$$

where θ_i and θ_f are the incidence and final angle of the scattered particle with respect to the surface normal. There are two parameters in this function μ and E_{int}/E_i, which can be adjusted to match the experimental observations.

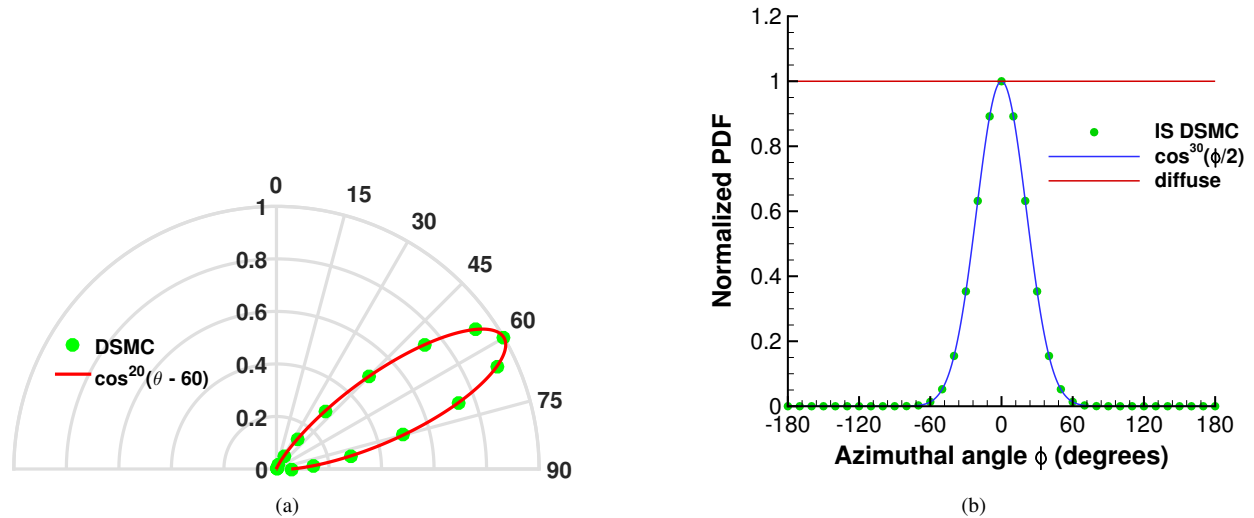3. *Angular distribution*

(a)

(b)

Figure 16: Representative angular distributions of products formed via impulsive scattering (IS) of a hyperthermal beam from a smooth surface. (a) Distribution in the plane containing the surface normal and the incident beam (in-plane): lobular distribution along the polar angle θ with $\theta_{peak} = 60^o$ and $n = 20$). (b) Distribution out of the plane containing the surface normal and the incident beam (out-of-plane): cosine power decay along the azimuthal angle ϕ with $m = 30$.

The angular distributions for impulsively scattered particles usually follow a lobular scattering with a peak on the opposite side of the surface normal from the incident beam.[28,36] The peak angle might be greater than the specular angle. The lobular pattern can be modeled using a cosine power law decay.

American Institute of Aeronautics and Astronautics

$$N(\theta) \propto \cos^n(\theta - \theta_{peak}) \tag{54}$$

where θ_{peak} is the location of the peak and the value of n determines the width of the distribution. Again both of these parameters can be chosen to match the experimental data. Fig. 16 (b) shows a lobular angular distribution for $\theta_{peak} = 60^o$ and $n = 10$.

The azimuthal angular distribution of the IS atoms is not expected to be uniform. Following the work of Glatzer $et\ al$[39], a cosine power law decay is used to approximate the out-of-plane scattering distribution.

$$N(\phi) \propto \cos^m\left(\frac{\phi}{2}\right) \tag{55}$$

The factor of 2 is introduced to ensure that the function remains positive within the range of the azimuthal angle: $(-\pi, \pi]$.

D. Non-thermal scattering model

Non-thermal scattering model is a generic model similar to the IS model described above but has more flexibility in terms of parameters to handle the wide range of cases where the products that scatter without accommodating to the surface temperature. It is noted that the CLL model can also be used to represent the non-thermally scattered particles, but this model provides higher flexibility.

1. VDF

The velocity distribution is represented using Gaussian distribution with a mean u_0 and a variance α following Rettner[37] similar to the IS model. u_0 and α are both free parameters which can be adjusted to match the experimentally observed distributions. However, unlike the IS model, u_0 is directly taken as an input instead of computing it based on the soft-sphere scattering model. In addition, there is no angular dependence of the VDF parameters.
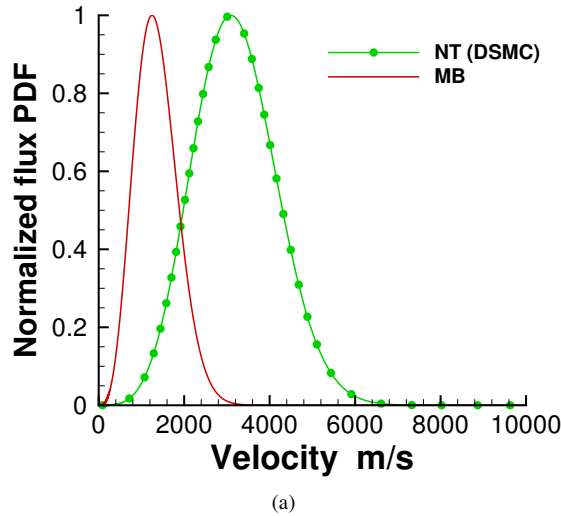

(a)

Figure 17: Representative flux PDF distributions of non-thermally (NT) scattered atoms from a smooth surface for a superthermal beam.

2. Angular distribution

Similar to the IS model, the polar angular distribution is expected to follow a lobular distribution represented using a cosine power law decay.

$$N(\theta) \propto \cos^n(\theta - \theta_{peak}) \tag{56}$$

θ_{peak} is the location of the peak and the value of n determines the width of the distribution. Again both of these parameters can be chosen to match the experimental data. Unlike the IS model, here the peak of the polar distribution is expected to be smaller than the specular angle.

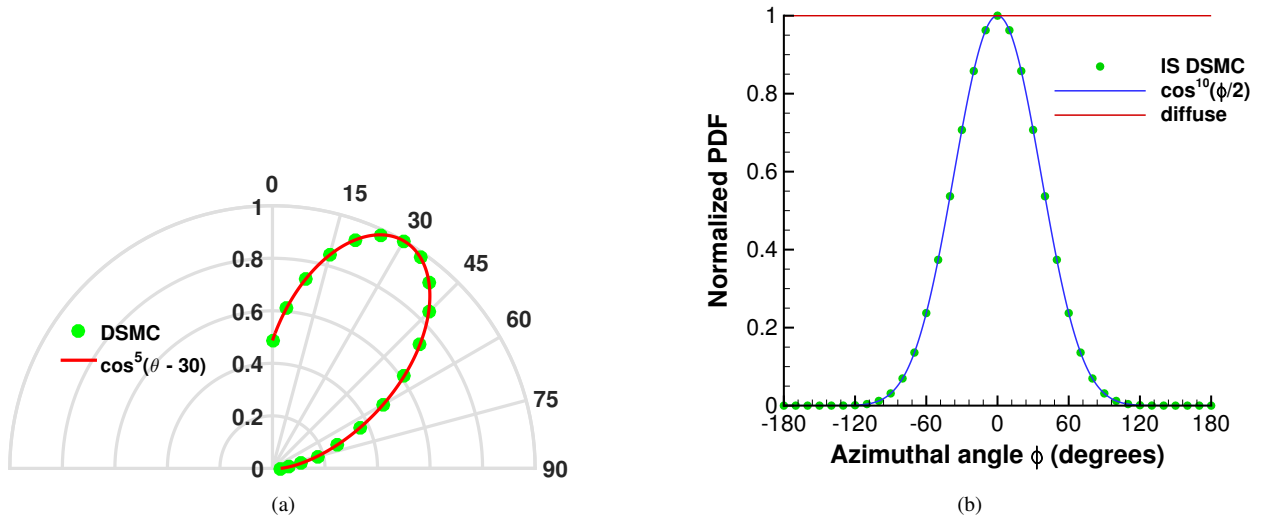American Institute of Aeronautics and Astronautics

Figure 18: Representative angular distributions of products formed via non-thermal (NT) scattering of a superthermal beam from a smooth surface. (a) Distribution in the plane containing the surface normal and the incident beam (in-plane): lobular distribution along the polar angle θ with $\theta_{peak} = 30^o$ and $n = 5$). (b) Distribution out of the plane containing the surface normal and the incident beam (out-of-plane): cosine power decay along the azimuthal angle ϕ with $m = 10$.

The azimuthal angular distribution is also represented using a cosine power law decay with its peak at an angle of zero following Glatzer et al.[39]

$$N(\phi) \propto cos^m \left(\frac{\phi}{2} \right) \tag{57}$$

The factor of 2 is introduced to ensure that the function remains positive within the range of the azimuthal angle: $(-\pi, \pi]$. Although the particles are scattered non-thermally, it is possible that the angular distribution might follow a diffuse distribution: cosine in polar direction and uniform in azimuth direction. This can be obtained by setting $\theta_{peak} = 0$, polar cosine power (n) as one and azimuth cosine power (m) as zero.

E. Combining scattering models

In many instances, a combination of scattering models may be required for representing the scattering of the same species over a range of conditions. For example, the physics of scattering at hyperthermal energies may be completely different from the scattering at thermal energies. Hence some provisions are required for using a combination of the available models to accurately capture the scattering over a wide range of conditions.

1. Energy threshold transition

Based on the energy of the incoming gas-phase atom/molecule the effective interaction experienced and the physics of scattering is completely different. They can be broadly classified into two regimes: (i) Thermal and (ii) Structural regime. When the energy of the molecule is relatively low compared to the thermal energy of the surface such that the effective interaction surface is relatively flat, then the interaction belongs to the thermal scattering regime. On the other hand, the structure regime corresponds to the case when the incident energy of the incoming particle are much higher compared to the surface thermal energies such that the surface vibrations are negligible. The effective interaction surface is rough at the atomic scale and the gaseous atom/molecule experiences the atomic structure of the surface atoms.

Thus, within the thermal regime scattering models such as the CLL, non-thermal and thermal models can be used to adequately represent the interaction of the gaseous species with the surface. The impulsive scattering model can be used to describe the gas-surface interaction in the structure regime. A continuous variation of the various scattering parameters as a function of energy is expected. However, in the absence of such detailed information simple transition between the different models can be used based on specified energy threshold.

Some reasonable threshold transition options are listed below.

i. One threshold: A single energy threshold value is specified along with two scattering models. Incident gas atoms/molecules with energy greater than the specified value is scattered based on the first model, while the

second model is used to scatter the particles with lower energies. This is the most basic model which abruptly transitions from one model to another.

ii. Two threshold - two models: Two energy threshold values are specified along with two scattering models. Particles with energy greater than the first threshold is scattered using the first scattering model, while particles with energy lesser than the second threshold is scattered using the second model. For particle energies in between the two energy thresholds a linear interpolation of the two models based on the incident energy is applied to get the final scattered properties. This creates a smoother transition between the different scattering models as compared to the one threshold model.

iii. Two threshold - three models: Two energy threshold values along with three scattering models are specified. Particles with energies greater than the first threshold, in between the two values and lesser than the second threshold are scattered using the first, second and the third model respectively. This is illustrative of a case where the physics of the transition from the structure to the thermal regime is much different from either of the two regimes.

2. Fraction based splitting

Another instance where a combination of gas-surface interaction models are required is when a fraction of products formed by a reaction mechanism scatters differently. For example, thermal mechanisms occurring when high energy particles are incident on the surface tends to have a small component that is non-thermal (super-thermal). This is termed as fraction based splitting of the particles under different scattering models. A generic way to implement this fraction based splitting is to specify any number of probability values (they must sum to 1), followed by an equal number of scattering models.

VII.   DSMC Input

The previous sections described in detail a generalized methodology to model finite-rate surface reaction mechanisms in DSMC. This section outlines the inputs required for the surface chemistry framework within the DSMC code.

When a gas-phase particle strikes the surface, all the possible GS reactions including that particular species is looped over. The probability for each reaction is calculated as described previously in Sec.IV. A random number is used to decide which reaction (if any) takes place, using the standard Monte Carlo technique for a sequence of events. At the end of each time step, all the possible PS reactions at each surface element is considered and performed without bias as described in Sec.V.

A.   Reaction format

The format of the surface reaction should follow the following conventions, in addition to the conventions for gas-phase reactions in SPARTA.

- At least one surface species must appear on each side of a reaction.

- Chemical elements must balance on both sides of a reaction.

- The number of like active sites must balance on both sides of a reaction.

- The number of surface species must balance on both sides of a reaction.

- The order of species on both sides of a reaction should be written as: gas species; mobile surface species; immobile surface species; and bulk species.

- An adsorption reaction is required for every adsorbed species.

- The phase of the species must be specified next to it within enclosed brackets (or parentheses) for both reactants and products.

    - For gas-phase species, the letter g should be used: (g).
    - For surface species, in addition to the phase, the site set should also be specified: (sp1,ss1).
    - For the bulk species, the phase must be provided: (bp1).
    - The bulk phase, surface phase, and surface site are order numerically starting from 1 in the order they were introduced.

American Institute of Aeronautics and Astronautics

– If no phase is specified, then it is assumed to be a gas-phase species.

- An empty surface site is represented by the letter E: E(sp1,ss1)

- Some reactions might contain catalytic species, which can be indicated by the use of letter c within curly brackets: {c}

B.   Reaction rate constants

The rate constant must be specified for each of the surface reactions. The most common form used for specifying the rate constant is the Arrhenius form with three parameters namely the pre-exponential factor (A), temperature exponent (β) and activation energy (E_a). However, some of the surface reactions can be represented in a more physical manner through the kinetics-based formulations for that particular type of reaction (GS, desorption and LH).[15] A summary is provided in Table 3.

Table 3: Different forms of specifying the reaction rate constants.

Reaction type	Rate formula	Specified parameters
Arrhenius	$AT'^{\beta} exp\left(-\frac{E_a}{RT}\right)$	A, β, E_a
GS	$\frac{\bar{v}}{4}\Phi_i^{-\nu_i} AT'^{\beta} exp\left(-\frac{E_a}{RT}\right)$	A, β, E_a
Desorption	$\Phi_i^{(1-\nu_i)} AT'^{\beta} exp\left(-\frac{E_a}{RT}\right)$	A, β, E_a
LH-2, LH-4	$\left[\bar{v}_{2D}\Phi_i^{(1.5-\nu_i)}\sqrt{A_v}\right] AT'^{\beta} exp\left(-\frac{E_a}{RT}\right)$	A, β, E_a

All the quantities must be specified in SI units. T' is a dimensionless temperature ($T' = T/1K$). The units of the pre-exponential factors can vary depending on the order of the reaction and the number of gas-phase, adsorbed and bulk-phase species present on the reactants and the products. $\bar{v}$ and $\bar{v}_{2D}$ are the mean thermal speed of the gas-phase species and a fully mobile surface species.

$$\bar{v} = \sqrt{\frac{8RT}{\pi M}} \qquad \bar{v}_{2D} = \sqrt{\frac{\pi RT}{2M}} \tag{58}$$

Φ_i is the site density of the surface where the ith surface reaction occurs. ν_i is the site density exponent equal to the sum of stoichiometric coefficients of all surface reactants. A_v is the Avogadro's number. In the case of adsorption, the sticking coefficient at zero surface coverage (required for the Kisluk's model to obtain $S(\theta)$) can be computed by:

$$S_0 = AT'^{\beta} exp\left(-\frac{E_a}{RT}\right) \tag{59}$$

C.   Specification of parameters

This section describes the specification for the structure of the input file for DSMC.

1.   System parameters

The following properties of the system must be specified first.

- Number of surface (N_{sp}) and bulk phases (N_{bp}).

- Name, surface fraction (θ_{sp_i}), site density (Φ_{sp_i}), and number of surface site sets ($N_{sp_i,ss}$) for each surface phase.

- Phase, surface fraction (θ_{sp_i,ss_j}), and number of species that can adsorb ($N_{sp_i,ss_j,a}$) for each surface site set.

- Name, volume fraction (ϕ_{bp_k}), density (ρ_{bp_k}), and number of species ($N_{bp_k,bs}$) for each bulk phase.

- Name, molecular weight in amu, molecular weight in kg, species weight, and charge for each surface species.

- Name, molecular weight in amu, molecular weight in kg, species weight, and charge for each bulk species.

2. Reaction parameters

Table 4: Parameters required for modeling gas-surface (GS) reactions.

Abbreviation	Reaction type	Example	Parameters	Description
AA	Associative adsorption	$A(g) + (s) \longrightarrow A(s)$	3	3(Rate constant)
DA	Dissociative Adsorption	$A(g) + \alpha(s) = \underbrace{B1(s) + B2(s)...}_{\alpha \text{ adsorbing products}} + \underbrace{C1(g) + C2(g)...}_{\beta \text{ gas-phase products}}$	$3 + \beta$ SM	3 (Rate constant) + β scattering models
LH1	Langmuir-Hinshelwood type 1	$A(g) + (s) + B(s) \longrightarrow AB(g) + 2(s)$ $A(g) + (s) + M(b) \longrightarrow AM(g) + (s)$	$3 + 1$ SM	3(Rate constant) + 1 scattering model
LH3	Langmuir-Hinshelwood type 3	$A(g) + (s) + B(s) \longrightarrow AB(s) + (s)$ $A(g) + (s) + M(b) \longrightarrow AM(s) + (s)$	3	3(Rate constant)
CD	Condensation	$M(g) + (s) \longrightarrow M(b) + (s)$	6	3(Rate constant) + 3(Kisliuk's model K_{eq})
AMD	Adsorption-mediated dissociation	$A(g) + \alpha(s) \longrightarrow \underbrace{B1(s) + B2(s)...}_{\alpha \text{ dissociation products}} + \alpha(s)$	$3 + \alpha$ SM	3(Rate constant) + α scattering models
ID	Impact dissociation	$A(g) \longrightarrow \underbrace{B1(s) + B2(s)...}_{\alpha \text{ dissociation products}}$	$3 + \alpha$ SM	3(Rate constant) + α scattering models
ER	Eley-Rideal	$A(g) + B(s) \longrightarrow AB(g) + (s)$	$3 + 1$ SM	3(Rate constant) + 1 scattering model
CI	Collision Induced	$A(g) + B(s) \longrightarrow B(g) + A(s)$	$5 + 1$ SM	3(Rate constant) + 2(m, n energy, cosine exponent) + 1 scattering model
		$A(g) + B(s) \longrightarrow A(g) + B(g) + (s)$	$5 + 2$ SM	3(Rate constant) + 2(m, n energy, cosine exponent) + 2 scattering models

Table 5: Parameters required for modeling pure-surface (PS) reactions.

Abbreviation	Reaction type	Examples	Parameters	Description
DS	Desorption	$A(s) \longrightarrow A(g) + (s)$	$6 + 1$ SM	3(Rate constant) + 3(K_{eq}^{des}) + 1 scattering model
LH2	Langmuir-Hinshelwood type 2	$A(s) + B(s) \longrightarrow AB(g) + 2(s)$ $A(s) + M(b) \longrightarrow AM(g) + (s)$	$3 + 1$ SM	3(Rate constant) + 1 scattering model
LH4	Langmuir-Hinshelwood type 4	$A(s) + B(s) \longrightarrow AB(s) + (s)$ $A(s) + M(b) \longrightarrow AM(s) + (s)$	3	3(Rate constant)
SB	Sublimation	$3C(b) + 3(s) \longrightarrow C_3(g) + 3(s)$	$3 + 1$ SM	3(Rate constant) + 1 scattering model

The equation of the reaction and their parameters are provided after the system parameters. Each reaction occupies two lines, the first line containing the equation of the reaction specified according to the conventions listed in Sec. VII.A. The second line provides the information about the type of mechanism, form of the reaction rate constant, followed by the parameters of the reaction. These parameters are used for performing the reactions (calculating probability or characteristic frequency) and determining the velocities of the gas-phase products (if any). The reaction type is specified by an abbreviation shown in the tables 4 and 5. The rate constant could be expressed in an Arrhenius form or the particular form shown in Table 3. Some of the reactions do not have a particular form and thus can be specified only in the Arrhenius form. The number of parameters required varies for each reaction type and is summarized in Table 4 for GS reactions and Table 5 for PS reactions.

VIII. Conclusion

In this paper, we have described the formulation and implementation of a general finite-rate surface chemistry framework in DSMC. The approach involves stochastically modeling the various competing reaction mechanisms occurring on a set of active sites. Within this framework, multiple surface phases can be specified allowing for the representation of composite materials similar to the formulation proposed by Marschall and Maclean for CFD.[15] Further each surface phase can contain multiple site sets which can be used to present heterogeneous surface materials like SiC.

The framework includes a comprehensive list of surface reaction mechanisms including adsorption, desorption, Eley-Rideal (ER), and different types of Langmuir-Hinshelwood (LH) mechanisms. It is possible to model both catalytic (oxygen formation) and surface altering (material removal by oxidation) reaction mechanisms. Based on the

presence of gas-phase species in the reactants, the reaction mechanisms are classified as gas-surface (GS) or pure-surface (PS) reactions. Since these two classes of reaction mechanisms have to be modeled as a part of different kernels within the DSMC framework, they are treated distinctly.

GS reactions are performed when the gas-phase particles strike the surface as a part of the *move* kernel. The modeling of GS reactions within DSMC involves the computation of the probability for each of the possible reactions. These probabilities are calculated from the specified reaction rate constant, properties of the incident gas-particle and the surface. Since the probabilities are obtained from rates, it is possible that the individual or cumulative probabilities exceed unity. In order to avoid any bias in such scenarios, a physically consistent multi-step procedure is presented for obtaining the reaction probability values.

PS reactions are carried out by looping over all the surface elements in parallel with the gas-phase collisions. DSMC modeling of PS reactions involve computing a characteristic frequency for each reaction. This characteristic frequency is a function of specified rate constants and surface properties. When multiple PS reactions are present, it is possible to introduce bias within the system. Two different algorithms for performing multiple PS reactions without bias were proposed and shown to accurately match the analytical solutions.

This work also presents various scattering models for accurately modeling both reactive and non-reactive scattering at a wide variety of regimes and scenarios. The different models available within this framework include CLL, thermal desorption, impulsive and non-thermal scattering models. In addition, this framework also allows for combining different scattering models to describe the scattering over a range of conditions. For each reaction, recommended models are proposed, but the framework is flexible to incorporate any specified model.

Based on the strength of the adsorbate-substrate bonding, the diffusion of the species on the surface might be important. The extreme limit is the case of mobile adsorption where the adsorbed species can freely move around the surface like a two-dimensional gas. Future developments will involve explicitly modeling surface diffusion of the adsorbed species based on the adsorbate-surface bond energy.

Finally, inclusion of this surface chemistry framework will introduce new kernels in the DSMC code and also alter some of the present kernels. Thus, the parallelization strategies used for the simple gas-phase DSMC code may need to be revised to account for inclusion of the surface chemistry framework (DSMC-SC). New parallelization strategies for DSMC-SC code will also be explored as a part of the future work.

American Institute of Aeronautics and Astronautics

A Bias introduced when total probability exceeds 1

This appendix outlines the importance of normalization when the total probability of a sequence of events becomes greater than 1. Without normalization, a bias will be introduced towards the initial events (reactions), even when the probability of each reaction is less than 1. Consider the following case with 5 events A, B, C, D, E, with the probabilities given in column 2 of Table A6.

Table A6: Un-normalized and normalized reaction probabilities of events

Events	Un-normalized probability (from rate constants)	Un-normalized probability cumulative	Un-normalized probability DSMC output	Normalized probability
A	0.40	0.40	0.40	0.20
B	0.30	0.70	0.30	0.15
C	0.20	0.90	0.20	0.10
D	0.60	1.50	0.10	0.30
E	0.50	2.00	0.00	0.25
Sum	2.00	-	1.00	1.00

Reactions in DSMC are performed using the standard Monte Carlo technique for a sequence of events:

- A random number is drawn for the reaction probability.
- The reaction probability is compared against a cumulative probability $\sum_{i=1}^{i=n} Prob(E_i)$, where n increases from 1 to the total number of events.
- When the value of the reaction probability is less than $\sum_{i=1}^{i=n} Prob(E_i)$, then the nth reaction is performed.

Using this methodology, and the un-normalized probability values, the actual occurrence of the five events are shown in column 4 of Table A6. The probability of events A, B, and C remains unaltered; the probability of D gets reduced to 0.1 and event E does not occur at all. Until the cumulative probability (column 3 of Table A6) remains less than 1, the probability of the events remains unaltered. When the cumulative probability exceeds 1, the probability of that particular event is truncated (such that the cumulative probability is equal to 1). The probability of the remaining events are zero. As one can clearly observe, a bias is introduced towards the initial events (reactions).

When the probability of each event is normalized by the sum of the un-normalized probability, we obtain the values given in column 5 of Table A6. These values retain the relative ratio of the original un-normalized provabilities, while having a cumulative probability of 1. This ensures that the relative probabilities of all the events remain unchanged and bias is prevented.

B Obtaining prescribed distributions

Although DSMC is very intuitive, sometimes sampling specific distributions for the different properties of the system, especially scattering properties from the surface, might not be straightforward. This section presents methods to sample prescribed distributions for the VDF and the angular distributions. These can be used to obtain the distributions described previously or any other user specified distributions.

A. VDF

In order to obtain the prescribed distribution for the velocity or energy of the particles scattered from the surface, it is first important to recognize the form of the prescribed distribution. In many instances instead of the VDF, the speed distribution function (SDF) or the distribution corresponding to the flux is specified. For example, the Maxwell-Boltzmann distribution has the following different forms when expressed as VDF, SDF or flux PDF.

$$VDF \propto exp\left(-\frac{mv^2}{k_bT}\right) \qquad SDF \propto v^2 exp\left(-\frac{mv^2}{k_bT}\right) \qquad flux\ PDF \propto v^3 exp\left(-\frac{mv^2}{k_bT}\right) \tag{60}$$

In this section, VDF is used as a generic term to describe any distribution relating to the velocity or energy of the particles. In order to obtain the correct distribution, the velocities of the scattering particles from the surface must be chosen based on the flux PDF.[40] The scattering of particles from the surface is similar to the effusive movement of gases through a plane. Hence, first the prescribed distribution must be properly converted into the flux PDF form before applying any of the standard Monte Carlo techniques to obtain the specified distribution. Based on the exact form of the distribution, corresponding techniques such as the inversion of the CDF or the acceptance rejection method can be used to obtain the final components of the velocities. These standard techniques for sampling the prescribed

distribution can be found in many texts including Bird[41], Shen[40], Frenkel and Smit[42] and Lesar.[43] While applying the acceptance rejection scheme for the VDF, it might be more efficient to use importance sampling[42] since most of the distributions involve an exponential function. The sharpness of the exponential function makes the random sampling very inefficient.

The process of converting the distribution into the flux form is straightforward in many cases, however care must be taken when the distribution is dependent on the angle of scattering. Also in some cases, the normal and the tangential distributions are available separately. In such a case, the tangential velocity distribution can be sampled directly while the normal component must be converted to the flux form.[40] If the inversion of the normal and tangential distributions are not straightforward, then it is recommended to convert them into a single combined distribution and apply the standard techniques to choose the total speed. Later the final angles can be used to obtain the separate components of the velocities.

B. Angular distribution

The most important feature to remember while sampling angular distribution is the presence of the sine of the polar angle in the expression for the solid angle.

$$d\Omega = sin(\theta)d\theta d\phi \tag{61}$$

θ is the polar angle while ϕ is the azimuth angle. Excluding this $sin(\theta)$ while sampling the distribution has been the source of confusion and error in the past.[44]

If the polar and azimuth distribution are not independent, the expression of the solid angle must be used directly within the sampling techniques. In the case where the two distributions are independent of each other, the azimuth sampling can be done without any additional factors. The polar sampling on the other hand must include the $sin(\theta)$ component.

$$f(\theta) = g(\theta) * sin(\theta) \tag{62}$$

where $g(\theta)$ is the required distribution in the polar direction, while $f(\theta)$ must be used within the sampling algorithms.

Acknowledgements

References

[1]Stephani, K. A., Goldstein, D. B., and Varghese, P. L., "A non-equilibrium surface reservoir approach for hybrid DSMC/Navier-Stokes particle generation," *Journal of Computational Physics*, Vol. 232, No. 1, 2013, pp. 468–481.

[2]Deschenes, T. R., Holman, T. D., and Boyd, I. D., "Effects of rotational energy relaxation in a modular particle-continuum method," *Journal of Thermophysics and Heat Transfer*, Vol. 25, No. 2, 2011, pp. 218–227.

[3]Swaminathan-Gopalan, K., Subramaniam, S., and Stephani, K. A., "Generalized Chapman-Enskog continuum breakdown parameters for chemically reacting flows," *Physical Review Fluids*, Vol. 1, No. 8, 2016, pp. 083402.

[4]Subramaniam, S., Swaminathan Gopalan, K., and Stephani, K. A., "Assessment of continuum breakdown for high-speed chemically reacting wake flows," *46th AIAA Thermophysics Conference*, 2016, p. 4434.

[5]Bergemann, F., "A detailed surface chemistry model for the DSMC method," *Rarefied Gas Dynamics*, 1995, pp. 947–953.

[6]Simmons, R. and Lord, R., "DSMC simulation of hypersonic metal catalysis in a rarefied hypersonic nitrogen/oxygen flow," *20th International Symposium on Rarefied Gas Dynamics*, AIP Publishing, 1996.

[7]Choquet, I., "A new approach to model and simulate numerically surface chemistry in rarefied flows," *Physics of Fluids*, Vol. 11, No. 6, jun 1999, pp. 1650.

[8]Gimelshein, S., Levin, D., and Collins, R., "Modeling of glow radiation in the rarefied flow about an orbiting spacecraft," *Journal of thermophysics and heat transfer*, Vol. 14, No. 4, 2000, pp. 471–479.

[9]Shumakova, A., Shevyrin, A., Bondar, Y., Kashkovsky, A., and Ivanov, M. S., "Effects of surface chemistry on high-altitude aerothermodynamics of space vehicles," *52nd AIAA Aerospace Sciences Meeting (National Harbor, Maryland, 2014)*, 2014.

[10]Molchanova (Shumakova), A. N., Kashkovsky, A. V., and Bondar, Y. A., "A detailed DSMC surface chemistry model," *AIP Conference Proceedings*, Vol. 1628, No. 131, 2014, pp. 131–138.

[11]Gallis, M. A., Torczynski, J. R., Plimpton, S. J., Rader, D. J., and Koehler, T., "Direct simulation Monte Carlo: The quest for speed," *AIP Conference Proceedings*, Vol. 1628, No. 1, 2014, pp. 27–36.

[12]LeBeau, G., "A parallel implementation of the direct simulation Monte Carlo method," *Computer Methods in Applied Mechanics and Engineering*, Vol. 174, No. 3-4, 1999, pp. 319–337.

[13]LeBeau, G. and Lumpkin Iii, F., "Application highlights of the DSMC Analysis Code (DAC) software for simulating rarefied flows," *Computer Methods in Applied Mechanics and Engineering*, Vol. 191, No. 6, 2001, pp. 595–609.

American Institute of Aeronautics and Astronautics

[14]Liechty, D. S., "Object-Oriented/Data-Oriented Design of a Direct Simulation Monte Carlo Algorithm," *Journal of Spacecraft and Rockets*, 2015.

[15]Marschall, J. and MacLean, M., "Finite-rate surface chemistry model, I: Formulation and reaction system examples," *42nd AIAA Thermophysics Conference*, 2011, p. 3783.

[16]MacLean, M., Marschall, J., and Driver, D., "Finite-Rate surface chemistry model, II: Coupling to viscous navier-stokes code," *42nd AIAA Thermophysics Conference*, 2011, p. 3784.

[17]Huffman, W., "The importance of active surface area in the heterogeneous reactions of carbon," *Carbon*, Vol. 29, No. 6, 1991, pp. 769–776.

[18]Lizzio, A. A., Jiang, H., and Radovic, L. R., "On the kinetics of carbon (char) gasification: reconciling models with experiments," *Carbon*, Vol. 28, No. 1, 1990, pp. 7–19.

[19]Sun, T., Fabris, S., and Baroni, S., "Surface precursors and reaction mechanisms for the thermal reduction of graphene basal surfaces oxidized by atomic oxygen," *The Journal of Physical Chemistry C*, Vol. 115, No. 11, 2011, pp. 4730–4737.

[20]Murray, V. J., Marshall, B. C., Woodburn, P. J., and Minton, T. K., "Inelastic and Reactive Scattering Dynamics of Hyperthermal O and O2 on Hot Vitreous Carbon Surfaces," *Journal of Physical Chemistry C*, Vol. 119, No. 26, 2015, pp. 14780–14796.

[21]Chorkendorff, I. and Niemantsverdriet, J. W., *Concepts of modern catalysis and kinetics*, John Wiley & Sons, 2006.

[22]Kisliuk, P., "The sticking probabilities of gases chemisorbed on the surfaces of solids," *Journal of Physics and Chemistry of Solids*, Vol. 3, No. 1-2, 1957, pp. 95–101.

[23]Kisliuk, P., "The sticking probabilities of gases chemisorbed on the surfaces of solidsII," *J. Phys. Chem. Solids*, Vol. 5, 1958, pp. 78–84.

[24]Somorjai, G. A., *Introduction to surface chemistry and catalysis*, John Wiley & Sons, 1994.

[25]Somorjai, G. A. and Li, Y., *Introduction to surface chemistry and catalysis*, John Wiley & Sons, 2010.

[26]Masel, R. I., *Principles of adsorption and reaction on solid surfaces*, Vol. 3, John Wiley & Sons, 1996.

[27]Weinberg, W., "Precursor intermediates and precursor-mediated surface reactions: General concepts, direct observations and indirect manifestations," *Kinetics of Interface Reactions*, Springer, 1987, pp. 94–124.

[28]Ertl, G., *Reactions at solid surfaces*, Vol. 14, John Wiley & Sons, 2010.

[29]Junell, P., Hirsimäki, M., and Valden, M., "Displacement of chemisorbed 12 CO from Pd {110} by adsorbing hot precursor 13 CO molecules," *Physical Review B*, Vol. 69, No. 15, 2004, pp. 155410.

[30]Lord, R., "Some extensions to the Cercignani–Lampis gas–surface scattering kernel," *Physics of Fluids A: Fluid Dynamics*, Vol. 3, No. 4, 1991, pp. 706–710.

[31]Lord, R., "Some further extensions of the Cercignani–Lampis gas–surface interaction model," *Physics of Fluids*, Vol. 7, No. 5, 1995, pp. 1159–1161.

[32]Abbott, H. L. and Harrison, I., "Dissociative chemisorption and energy transfer for methane on Ir (111)," *The Journal of Physical Chemistry B*, Vol. 109, No. 20, 2005, pp. 10371–10380.

[33]Abbott, H. L. and Harrison, I., "Activated dissociation of CO2 on Rh (111) and CO oxidation dynamics," *The Journal of Physical Chemistry C*, Vol. 111, No. 35, 2007, pp. 13137–13148.

[34]Gillespie, D. T., "A general method for numerically simulating the stochastic time evolution of coupled chemical reactions," *Journal of computational physics*, Vol. 22, No. 4, 1976, pp. 403–434.

[35]Goodman, F. O., "Simple model for the velocity distribution of molecules desorbed from surfaces following recombination of atoms," *Surface Science*, Vol. 30, No. 3, 1972, pp. 525–535.

[36]Goodman, F. O., *Dynamics of gas-surface scattering*, Elsevier, 2012.

[37]Rettner, C. T., "Reaction of an H-atom beam with Cl/Au(111): Dynamics of concurrent EleyRideal and LangmuirHinshelwood mechanisms," *The Journal of Chemical Physics*, Vol. 101, No. 2, 1994, pp. 1529.

[38]Alexander, W. A., Zhang, J., Murray, V. J., Nathanson, G. M., and Minton, T. K., "Kinematics and dynamics of atomic-beam scattering on liquid and self-assembled monolayer surfaces," *Faraday discussions*, Vol. 157, 2012, pp. 355–374.

[39]Glatzer, D., Häger, J., Fink, M., and Walther, H., "Rotationally excited NO molecules incident on a graphite surface: in- and out-of-plane angular distributions," *Surface Science*, Vol. 374, No. 1, 1997, pp. 169–180.

[40]Shen, C., *Rarefied gas dynamics: fundamentals, simulations and micro flows*, Springer Science & Business Media, 2006.

[41]Bird, G., *Molecular Gas Dynamics and the Direct Simulation of Gas Flows*, Oxford University Press, Oxford, 1994.

[42]Frenkel, D. and Smit, B., *Understanding molecular simulation: from algorithms to applications*, Vol. 1, Academic press, 2001.

[43]LeSar, R., *Introduction to computational materials science: fundamentals to applications*, Cambridge University Press, 2013.

[44]Greenwood, J., "The correct and incorrect generation of a cosine distribution of scattered particles for Monte-Carlo modelling of vacuum systems," *Vacuum*, Vol. 67, No. 2, 2002, pp. 217–222.